Monitoring Forest Fire using Geo-Spatial Information Techniques and Spatial Statistics: One Case Study of Forest fire in Margalla Hills, Islamabad, Pakistan

Aqil Tariq
Wuhan University
Hong Shu (shu_hong@whu.edu.cn)
Wuhan University https://orcid.org/0000-0003-2108-1797
Saima Siddiqui
University of the Punjab

Research

Keywords: Forest fire, Geospatial analysis, Delta normalized burn ratio, Determining factors, Fire severity.

Posted Date: August 25th, 2020

DOI: https://doi.org/10.21203/rs.3.rs-60874/v1

Monitoring forest fire using Geo-spatial information techniques and spatial statistics: one case study of forest fire in Margalla Hills, Islamabad, Pakistan

Aqil Tariq[1], Hong Shu[1], Saima Siddiqui[2]*

[1]State key laboratory of Information Engineering in Surveying, Mapping and Remote Sensing (LIESMARS) Wuhan University, 430079, Wuhan, China.

[2]Department of Geography, University of the Punjab, Lahore, Pakistan.

Corresponding Authors

Hong Shu (Shu_hong@whu.edu.cn)

State key laboratory of Information Engineering in Surveying, Mapping and Remote Sensing (LIESMARS) Wuhan University, 430079, Wuhan, China.

Abstract

Background

Understanding the spatial patterns of forest fires is of key importance for fire risk management with ecological implications. Fire occurrence, which may result from the presence of an ignition source and the conditions necessary for a fire to spread, is an essential component of fire risk assessment.

Methods

The aim of this research was to develop a methodology for analyzing spatial patterns of forest fire danger with a case study of tropical forest fire at Margalla Hills, Islamabad, Pakistan. A geospatial technique was applied to explore influencing factors including climate, vegetation, topography,

human activities, and 299 fire locations. We investigated the spatial extent of burned areas using Landsat data and determined how these factors influenced the severity rating of fires in these forests. The importance of these factors on forest fires was analyzed and assessed using logistic and stepwise regression methods.

Results

The findings showed that as the number of total days since the start of fire has increased, the burned areas increased at a rate of 25.848 ha / day ($R^2 = 0.98$). The average quarterly mean wind speed, forest density, distance to roads and average quarterly maximum temperature were highly correlated to the daily severity rating of forest fires. Only the average quarterly maximum temperature and forest density affected the size of the burnt areas. Fire maps indicate that 22% of forests are at the high and very high level (> 0.65), 25% at the low level (0.45-0.65), and 53% at the very low level (0.25 – 0.45).

Conclusion

Through spatial analysis, it is found that most forest fires happened in less populated areas and at a long distance from roads, but some climatic and human activities could have influenced fire growth. Furthermore, it is demonstrated that geospatial information technique is useful for exploring forest fire and their spatial distribution.

Keywords: Forest fire; Geospatial analysis; Delta normalized burn ratio; Determining factors; Fire severity.

1 Backgrounds

Forest fires appear unavoidable in the natural world and they play a vital role in the regeneration of flora and the change of ecosystems. Nonetheless, unregulated forest fires may have detrimental environmental and local impacts. This is because these fires not only property and harm human life but also endanger ecosystem permanency. There has been a growing increase in the amount and intensity of forest fires across the world over the last decade. This phenomenon raises public concern about the environmental and socio-economic impacts of forest fires.

According to a 2015 report by the Ministry of Climate Change and Capital-Development-Authority (CDA), Islamabad, Pakistan has a forest cover of around 5.2% of its geographical region (Islamabad 2015). Due to climate change and increased human economic activity, forest fires in this country in recent years have become a major environmental disaster that has burned large quantities of natural resources, destroyed the soil and caused air pollution (Schoennagel et al. 2004; Krebs et al. 2010). In addition to the altering human activities in land use, prolonged dry weather with unusually high temperature raises the number of fires across a significant part of Islamabad. Because of the major effect of forest fires have on habitats and forest fire prevention, socio-economic conditions, and suppression have become a shared concern of researchers and governments around the world. In order to develop successful fire prevention and suppression plans, regional-scale maps of fire susceptibility need to be created (Oliveira et al. 2012; Fusco et al. 2018). These maps not only promote the appropriate distribution of resources required for fire prevention and suppression but also provide considerable support for land use planning tasks (Parks et al. 2011; Valdez et al. 2017).

Recent developments in the RS & GIS have tremendously assisted the task of developing maps of forest fire susceptibility (Cortez 2006; Khalid and Saeed Ahmad 2015; Rtificial and Pproach

2015). GIS allows for the easy execution of the tasks of recording, evaluating, handling and displaying geographic data. The forest fire threat in an area can be evaluated taking into account several inducing factors including climate, vegetation, topography and human activities. The spatial associations between those variables and the regional historical fire record can be used to create data-driven models that perform accurate predictions of fire susceptibility for all areas of the world. Researchers have focused on the contribution of vegetation type and continuity, fire environment and topographic factors that influence the fire spread rate and period of favorable conditions, and human involvement in fire suppression and extinguisher (Viegas et al. 1999; Samanta et al. 2011; Calkin et al. 2014).

Previous studies have analyzed factors influencing long term forest fire, burning threat and risk in Asia mostly at the local level and also at the national level (Pew and Larsen 2001; Bonazountas et al. 2007; Duane and Brotons 2018). They used various statistical approaches, simulations, and algorithms to assess the impact of climatic, and environmental influences. For example, in northeast Iran's Golestan forest region,(Abdi et al. 2016) used a multiple-regression model to establish associations between forest managing variables and forest fire occurrence, with a clear positive association (up to 70%) between fire period and low forest road number, barrier and forest organization channel quarry plans (Mohammadi et al. 2014).

In this study, we describe the spatial pattern of forest fire and factors influencing the occurrence of fire on a large scale and model the probability of occurrence of fire in Pakistan where this phenomenon is recurrent. The assessment of the incidence of fire at this scale may provide guidance for the preparation and implementation of fire prevention measures, in particular the design of forest management strategies adapted to different environmental conditions. In this study we assess and compare the relative contribution of climate, vegetation, topography, and human

activity to the incidence, scale, and burnt area of fire in a northern Punjab, Pakistan. Pakistan is filled with a range of edaphic, physiographic, climatic and wildlife differences (Department 1927; Cortez 2006; Tanvir and Mujtaba 2006; Syeda Ifrah Ali Abidi and Junaid Noor 2013; Khalid and Saeed Ahmad 2015). Many fires are scattered across a zone of roughly 11,603 hacters. From 2002 to 2011, 75% of the forest fires last for about1-4 hours and 15% for 4-8 hours (Khalid and Saeed Ahmad 2015). The main aim of this research is to identify the spatio-temporal changes in burnt area using Landsat 7 (ETM+) and 8(OLI/TIRS) data. We used modeling and predicting the fire ignition and size distribution daily and yearly. The geospatial techniques were used to identify burned areas and compare forest fire aspects with various variables including climate, vegetation conditions, topography and human activities from 2005-18. Statistical analysis was used to identify susceptibility of forest fires dependent on the important effect on fire severity dynamics in the forests of Margalla hills, Islamabad, Pakistan.

2 Materials and Methods

2.1 Study Area

This study was conducted in Margalla Hill, Islamabad capital of Pakistan (33° 043'N and 72° 055'E (Fig. 1)). Margalla Hills are situated on the north-eastern part of the Islamabad Capital Territory, Pakistan (Blocks 2007). Among Pakistan's naturally significant safe areas, Margalla national park contains a scrub tree environment associated with biodiversity. It is located in the north-eastern part of the capital city of Islamabad, Punjab and occupies nearly 15,883 hectares (1994). This study area extends to the hills of Murree in the east and the Wah Cement Industries in the west. In the west and northwest, it is surrounded by the capital border beyond which the Haripur district Khyber Pakhtun Khwa (KPK) is located (Khalid and Saeed Ahmad 2015). The natural climate is

subtropical with mild summers and winters. The average maximum summer temperature of the region is 34.3 ^{o}C and the average annual rainfall is 1200 mm per year with less snow fall in winter (Muhammad Ibrar Shinwari and . 2000). There is no industrial operation to clear trees and the population density level is very small i.e. less than 15 people per km^2 in the study area (Khalid and Saeed Ahmad 2015).

Each year, Margalla Hills experience fire incidents mainly in the Chir pine (Pinus roxburghii Sarg.) owing to their dry indicators as a litter over the field having raisin in it and is often named as "hot wood." Incidents of fire arise because of two primary causes i.e. normal and anthropogenic behavior. Rock weathering, lightening and hot environment are the normal means of forest fire rising and spreading in the area, while human presence and disturbance in the woodland region and cause of woodland vegetation burning falls in second place based on reports of fire incidents (Brooks and Lusk 2008; Iqbal et al. 2013; Collen et al. 2015).

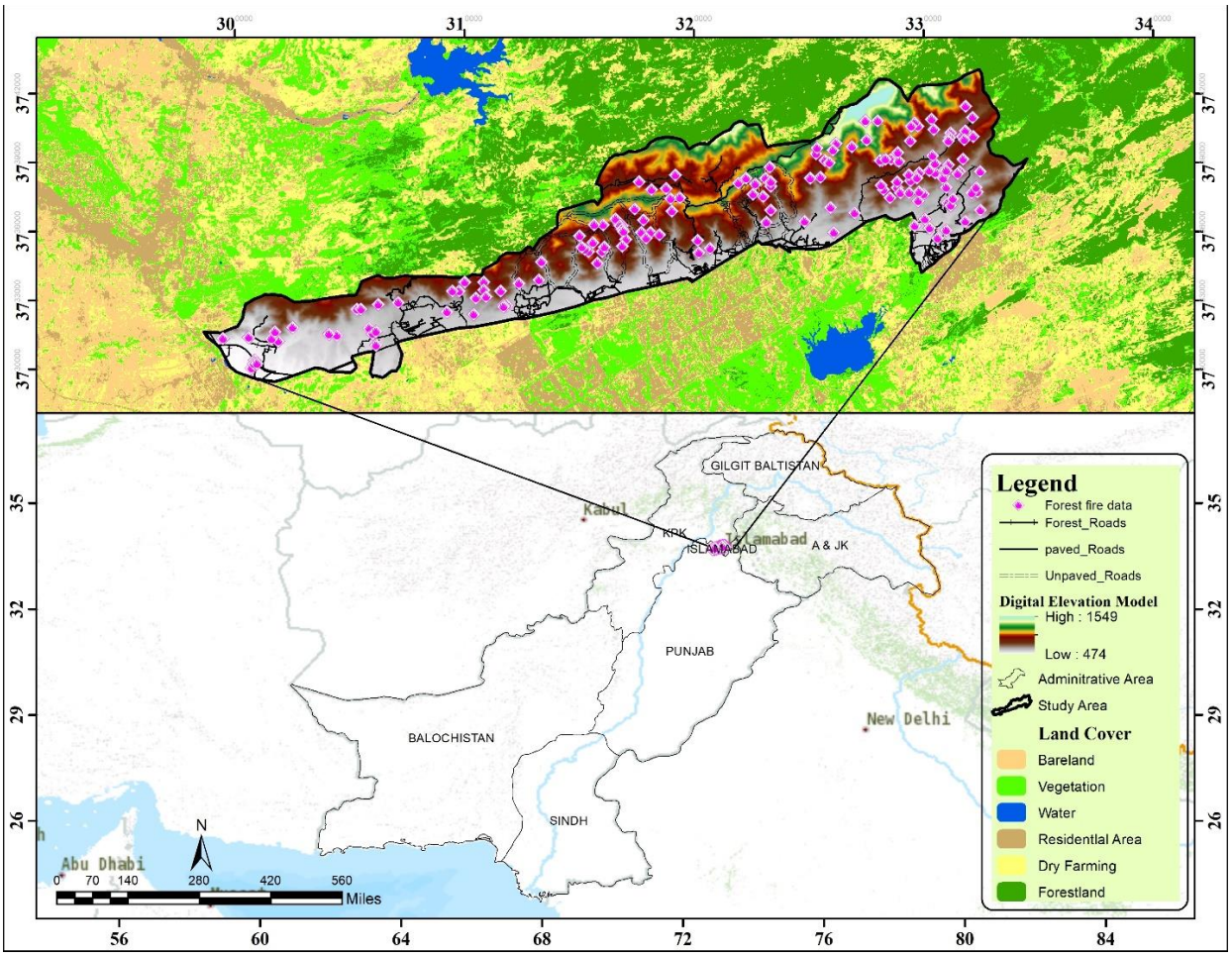

Insert Fig. 1. Geographical location of study area, red points referring to the spatial distribution of most forest fire occurrence area.

2.2 Forest fire occurrence data

The geo-database of forest fire is founded on a data archive, covering completely recorded forest fires during various field surveys conducted from 15th June 2005 to 12th July 2018 (14 consecutive years) (Table 1). A total number of 299 fires were recorded in the Margalla Hills, 30 of which were lightning-ignited as indicated in Fig.1. Small patches origins of the fire are mostly unknown. Each fire statement included numerous variables such as location of the explosion, time, day of ignition, final burned area, environment and approximate reason. All these forest fires erupted in May, June and July showing that summer is the main fire season in the study area.

Insert Table 1. Data of forest fires occurring from 2005 to 2018 on Margalla hill.

Year	Number of fires	Duration (Cumulative no of days)	Cumulative days of fire occurrence	Burnt areas (ha)	Cumulative Burnt areas (ha)	Field survey generate map data	Cumulative Burnt area (Field survey data	Burnt area (percentage)
2005	22	23	23	2476.08	2476.08	2630.63	2630.63	15.58
2006	12	9	32	981	3457.08	1023.53	3654.17	6.17
2007	23	21	53	2554.38	6011.46	2430.36	6084.53	16.08
2008	33	23	76	3478.5	9489.96	2760.35	8844.88	21.90
2009	22	20	96	2119.86	11609.82	1911.34	10756.23	13.34
2010	11	8	104	923.58	12533.4	972.21	11728.44	5.81
2011	15	25	129	341.82	12875.22	358.46	12086.90	2.12
2012	19	33	162	234.72	13109.94	254.82	12341.72	1.47
2013	26	37	199	1017.81	14127.75	987.54	13329.27	6.40
2014	36	38	237	3141.99	17269.74	3051.34	16380.61	19.78
2015	23	36	273	3275.19	20544.93	3125.55	19506.17	20.62
2016	22	18	291	350.82	20895.75	315.54	19821.71	2.20
2017	17	26	317	3358.8	24254.55	2935.93	22757.65	21.14
2018	18	20	337	1557.81	25812.36	1491.63	24249.28	9.80

2.3 Ancillary data

The main source of digital data correlated to all factors influencing the forest area was the capital development authority (CDA), Islamabad Pakistan. The maps are two-dimensional (2D) and three-dimensional (3D) data and topographic maps. Meteorological data including precipitation, humidity, mean daily wind speed, mean daily maximum and minimum temperature were obtained from Pakistan Meteorological Department (PMD), Islamabad, Pakistan. ArcGIS 10.6 was used to perform both digital data analysis and spatial modeling. A Geodatabase was created for residential areas, boundary lines, paved/unpaved, forest road and residential road network. All spatial data are available at a scale of 1:20,000, as a representation of Universal-Transverse-Mercator (UTM), zone 43 and as WGS84 Datum.

2.4 Remote sensing data and processing

We obtained Landsat 7 (ETM+) data for the years 2005 to 2012 and Landsat 8 (OLI + TIRS) data for the years 2013 to 2018. All available Landsat (ETM+ OLI/TIRS) data between 2005 to 2018 (cloud cover 0-3%) was obtained from USGS-EROS (https://www.usgs.gov/). Later, Landsat 7 and 8 images were used as inputs to generate a Normalized Differentiated Vegetation Index (NDVI), Normalized Burn Ratio (NBR) and Delta Normalized Burn Ratio (dNBR) images. From 2005 to 2018 Landsat images were used, one image from pre-fire and one from post-fire were analysed. Landsat ETM+ and OLI/TIRS images with 08 bands were used to estimate pre and post fire burned area from 2005 to 2018. Normalized differentiate vegetation index (NDVI), Normalized burned ratio (NBR) and delta normalized burn ratio ($dNBR$) areas were identified using ERDAS imagine 2016.

2.5 Burned area mapping

Burnt area analysis was done separately using Landsat 7 and Landsat 8 datasets, and all the pixels identified as burned were compiled into a composite image. Different burned area maps were created from the images acquired by Landsat sensors from May 2005 to July 2018. The maps were then mixed at 10-meter resolution.

We collected samples from ETM+ and OLI images from the top of the atmosphere across the study area. While past studies had shown that surface reflection, data would remove differences due to atmospheric effects (Ouaidrari and Vermote 1999; Masek et al. 2006; Roy et al. 2014, 2016; Skakun et al. 2018) At the time of test, not all of the sensors examined in this analysis had surface reflectance data stored in the USGS Earth Explorer, the primary objective of which was the application of this sample.

Hence, top-of-atmosphere (TOA) correction methods were used; precisely, for Landsat ETM+ and OLI, radiometric correction to Level 1 TOA (Ouaidrari and Vermote 1999; Storey et al. 2014).

Throughout the ENVI 5.4, both data extraction and pre-processing of images (conversion of DN to reflection) was performed. Stacking layers requires merging bands to create a single multispectral image. Analysis method was used to clip area of study. Burned areas were marked by the disparity between each date and the base mosaic in the value of two satellite indices. For each year, two maps were created from ArcGIS 10.6 software, using Landsat images and exporting the maps. Because during a particular period, after obtaining two desired images (pre and post), an algorithm was performed on the satellite-images to measure burned areas and also to match the ancillary data received by Islamabad, CDA (Lesmeister et al. 2019).

Three indices were used to measure burned area from Landsat data. The Normalized Differentiate Vegetation Index (NDVI) is the most frequently used band ratio in ecological science and widely used in rangeland experiments, though with differing degrees of performance. NDVI is a plant predictor which was considered to be a valuable covariate in DSM (Mulder et al. 2011). This measure has values varying from -1 to 1 (Jensen and Lulla 1987). The typical green vegetation range is from 0.2-0.8. The ratio between $(Band_{Red} - Band_{NIR})$ and $(Band_{Red} + Band_{NIR})$ is called the NDVI (1)(Escuin et al. 2008).

$$NDVI = \frac{B_{RED} - B_{NIR}}{B_{RED} + B_{NIR}} \quad (1)$$

Where B_{REd} denotes 0.63-0.69μm wavelengths, and where B_{NIR} involves wavelengths of 0.76-0.86μm. We required two images for the calculation of NBR following equation 2 (Escuin et al. 2008). NBR was measured from an image shortly before burning, and a second NBR is estimated for an image just after burning.

$$NBR = \frac{B_{NIR} - B_{SWIR}}{B_{NIR} + B_{SWIR}} \quad (2)$$

Where B_{NIR} denotes 0.76-0.90μm wavelengths, and where B_{SWIR} involves wavelengths of 2.09-2.35 μm. The delta-normalized-burn-ratio ($dNBR$) was calculated using equation 3 (Veraverbeke et al. 2010). The NBR was used for determining the severity of a fire. Burned frequency and severity are determined by differentiating between these two index layers:

$$dNBR = NBR_{Pre-fire} - NBR_{Post-fire} \quad (3)$$

High values range of $dNBR$ indicates more severe damage and negative range values suggest decreased vegetation productivity after-fire. "Non-processing zones" contains portions of the background covered by fog or haze or wet areas. Processed satellite data and the CDA field data were grouped in two clusters. The first cluster, shows calculated indices of NDVI, NBR and dNBR and second cluster used ground field derived data including NBR-FD and dNBR-FD. Correlation matrices between Landsat image and CDA field data were estimated and all variables were performed in R software. Correlations having absolute values greater than 0.6 were tallied within the field and image categories were named by sensor type and strength of the Pearson correlation coefficient.

2.6 Spatial analysis

Environmental factors were obtained from the ALOS-PALSAR Digital Elevation Model (DEM) with a 10m utilizing surface analysis functions. The DEM was obtained at a spatial resolution of 12.5m from Synthetic-Aperture-Radar (SAR) data from the L- band. In this analysis the DEM has been resampled (coarse gridded) to 10m spatial resolution. Terrain attributes, i.e. slope, aspect, curvature plane, Terrain Position Index (TPI) and Topographic Wetness Index (TWI), were obtained from the DEM using SAGA-GIS. Forest density was estimated using Landsat images of

30m spatial resolution. The normalized differentiate vegetation index (NDVI), using sub-pixel classification and converted into $10m^2$ spatial resolution according to all remote sensing data.

Various GIS and RS functions were used to model climatic factors (V. Radha Krishna Murthy 2004; Bhunia et al. 2011; Samanta et al. 2011). Mean daily meteorological data were gathered from the meteorological stations. These data were extrapolated to measure meteorological layers with a cell size of $10m^2$. To this purpose, a multiple-regression approach has been employed. Each variable was linked to the corresponding coordinates and elevation data, including mean maximum temperature, mean minimum temperature, mean relative humidity, wind speed, and rainfall. To obtain the smallest discrepancy between observable data and negative simulated data, various configurations have been evaluated. X, Y coordinates and every cells middle Z values were obtained by developing a DTM array of $10m^2$. An algebraic equation was used by examining all variables of meteorology and then interpolated methods were used in spatial analyst tool in Arc GIS 10.6 software package.

Then, various factors induced by anthropogenic activities were evaluated, comprising of the residential area, paved and unpaved/dirty roads. The distance from forest road maps were generated through connectivity and spread utilities (Cutler et al. 2007), while the kernel density function was applied to prepare the population density layer (Table 2).

Insert Table 2. List of climatic, vegetation, topography, and human activities concerning the fire occurrence and its sources.

Type of data	Environmental covariates	Sources
Remote sensing	Landsat 7	Landsat
	Landsat 8	Landsat
Forest density	Normalized differentiate vegetation index (NDVI)	Landsat
DEM	Elevation (m)	ALOSPALSAR

Slope	Slope degree	ALOSPALSAR
Aspect	Aspect degree	ALOSPALSAR
Plan curvature	Direction of slope	ALOSPALSAR
TWI	Topographic wetness index (TWI)	ALOSPALSAR
TPI	Terrain position index (TPI)	ALOSPALSAR
Temperature	Mean monthly quarterly temperature	PMD
Precipitation	Mean monthly quarterly precipitation	PMD
Relative humidity	Mean monthly quarterly and annual humidity	PMD
Wind speed	Mean monthly, quarterly and annual wind speed	PMD
Population density	Population density (people/km^2)	CDA
Residential distance	Distance to the residential (m)	OSM
Paved road distance	Distance to the paved road (m)	OSM
Unpaved / Dirty road distance	Distance to the dirty road (m)	OSM
Forest road distance	Distance to the forest road (m)	OSM

2.7 Statistical analysis

The severity of forest fire was seen from the beginning to the end of the fire across the entire burned field. Total burned extents were assessed against duration (days). The time for burning was calculated from this curve by applying a logistic function to the total burned areas (G) versus duration (t, hours) as shown in equation 4 (Abdi et al. 2018).

$$\mathrm{G} = \frac{F_x}{1 + exp[a(t-b)]} \quad (4)$$

Where F_x is the maximum burned area, b is the duration/time to reach 50% of all total burned areas and a is a value calculated by an iterative process of optimization to reduce the observed minus the predicted value. The periods for 5%, 10%, 90% and 95% were also calculated by interpolation and were referred to as A5, A10, A90 and A95, respectively.

The zonal statistics method was used to measure the mean values of climatic, vegetation, topography and human activities for each fire area. Therefore the stepwise multiple-regression approach (FAO 2009) was supported out to invent the association between predictors and dependent which was compiled in the R Package software. The four factor variables (climatic, vegetation, topography and human activities) were connected with the dependent variables (forest fire severity) in the model. Variables with a greater correlation were added, and lower correlation variables were discarded. Ultimately, numerical models of susceptibility to forest fire were created. Spatial maps of susceptibility to forest fire were produced in a raster format based on these models. Later these maps were divided into three groups using the equal interval process.

3 Results and discussion

3.1 Burned area mapping

Fig.2 shows the delta Normalized Burn Ratio maps of Margalla Hills in different distinguished colors from 2005 to 2018 respectively. It can be observed that delta normalized burned area is concentrated in the eastern, central and southern area and had been expanding from 2005 to 2018. The proportion of delta NBR increased from 1.4% to 21.9% in 2005 to 2018. Delta normalized burn ratio areas are mainly located near residential and road network covered areas. However, no changes have been detected in the north and northwestern vegetative cover areas, since they are located in the mountains. Similarly, no case was reported near water bodies. NBR, dNBR, NBR-FD and dNBR-FD burn severity indices indicated higher proportion of significant correlation greater than 0.6 within the variables (Table 3). Comparison of NBR, NBR-FD, dNBR and dNBR-FD showed that dNBR worked in a general way. After comparing NBR and dNBR for several individual fires, NBR appeared to correlate better to field attributes when the post-fire image

captured immediate post fire effects. After several weeks have elapsed since burning, dNBR appeared to produce the better correlations.

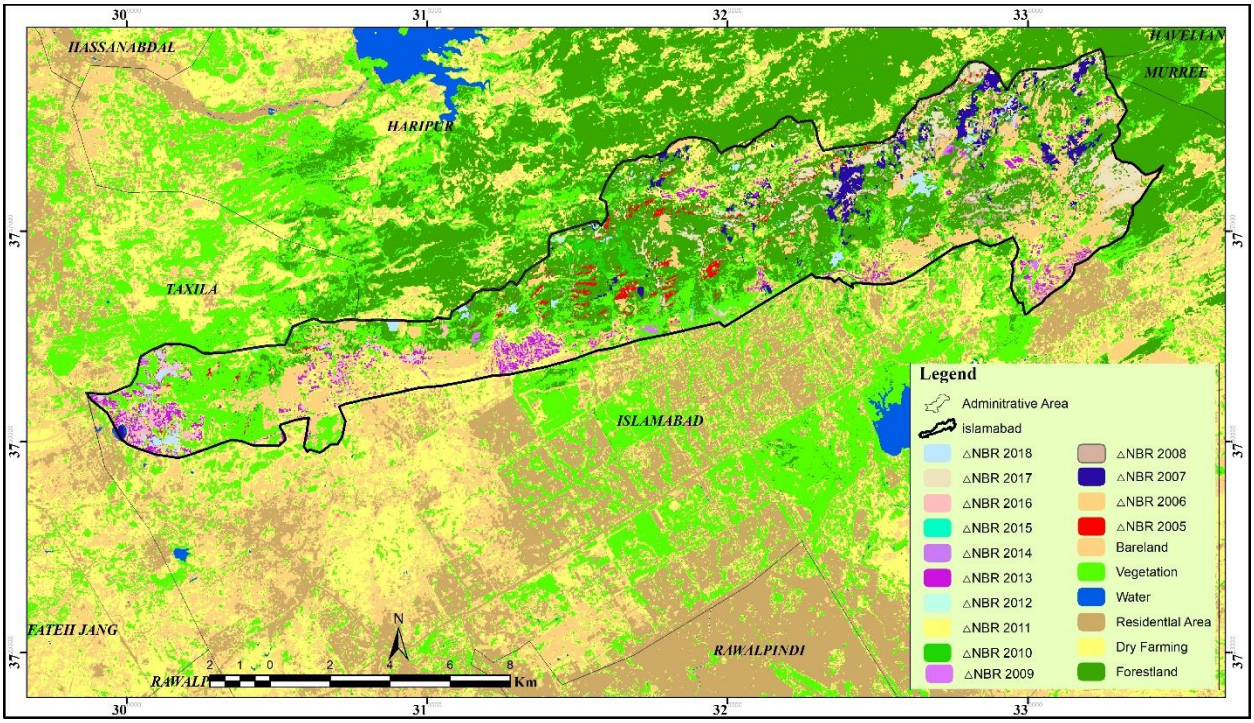

Insert Figure 2. Delta normalized burn ratio map of Margalla hills varying annually.

Insert Table 3. Pearson correlation between satellite derived and ground based derived results.

	NBR	dNBR	NBR-FD	dNBR-FD
NBR	1.0000	0.0695	0.0344	0.9997
dNBR	0.0695	1.0000	0.9874	0.0715
NBR-FD	0.0344	0.9874	1.0000	0.0385
dNBR-FD	0.9997	0.0715	0.0385	1.0000

3.2 Climatic, vegetation, topography, and human activities concerning forest fire.

Forest-fires are a major contemporary challenge to valuable forest resources in the Margalla region, Islamabad. Nearly 25812.36 hectares forest area was burned during May 2005 to July 2018. The scale of the fire patches was estimated as 0.3 to 2523 hectares (Fig. 2). In general, during less than a month, almost 7% of the trees were burned. Logistic model findings show that the burned

areas have increased at a pace of 25.848 ha/day (Fig. 3a; $R^2 = 0.98$). Furthermore, the figures show that approximately 50% of the overall region was burned over a period of 25 days. the remaining 50% area was burned during the following 13 days period and 1707.3 ha/year (Fig. 3b; $R^2 = 0.97$). The rate the fire extent increased at the end of the period revealed that fire exploitation and prevention operations were unsuccessful.

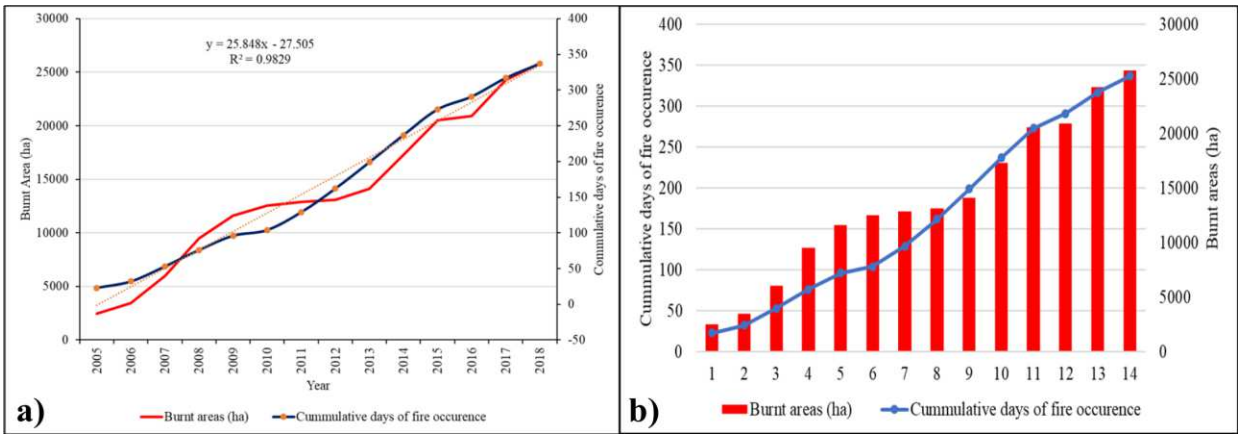

Insert Fig. 3. a) Logistic regression comparison between burnt area and fire duration in the experimental region and b) Total days of incidence of fire against burnt region (total cumulative days).

Insert Table 4. Stepwise regression and significant factors of forest fires causing.

Factors	Sig.	F.	R^2
Fire durability			
Forest density	0.0030	11.32	81.27
Average warmest windspeed quarter (AWWQ)	0.0432	5.01	59.81
Average warmest quarterly min temperature (AWQmiT)	0.0210	21.93	55.46
Average warmest quarterly max temperature (AWQmaT)	0.0023	24.64	58.23
Distance to roads	0.0002	8.96	82.64
Topographic wetness index (TWI)	0.0001	5.34	44.59
Terrain position index (TPI)	0.0001	11.23	60.94
Burnt area			
Average warmest quarter min temperature (AWQmiT)	0.006	9.1	27.48
Average warmest quarter max temperature (AWQmaT)	0.007	8.3	84.58
Forest density	0.001	132.01	82.24
Population density	0.002	4.34	78.34
Residential distance	0.003	8.33	81.34

Insert Table 5. Long-term estimates of climate parameters during the forest fire period (1990–2018).

Climatic variables	Average statistics for May, June and July	
	Long term	2005-2018
Average warmest quarter min temperature (AWQmiT)	18.24	23.04
Average warmest quarter max temperature (AWQmaT)	28.52	36.23
Average warmest quarterly precipitation (AWQP)	98.23	116.22
Average warmest windspeed quarter (AWWQ)	7.30	13.32
Average warmest relative humidity quarter (AWRQ)	72.34	55.32
Frequency of precipitation (day)	11.23	4.79

The effects of the climatic, vegetation, topographic and human activities on frequency of forest fire occurrence are seen in Table 4 on stepwise regression. The initiation and spreading of a fire are primarily influenced by the surface fuels 'water content, the trees' moisture content, and the wind direction. The litter quality content to be measured is given by different limitations e.g. air temperature, and precipitation (FAO 2009). Climate parameters were prepared for the fire amount in the Margalla Hills. During the study period from June 2005 to July 2018 the average warmest quarterly maximum temperature (AWQmaT) was observed approximately 7.84^{o}C that is higher than the long-term AWQmaT from 1990 to 2018. Average warmest quarterly minimum temperature (AWQmiT) was approximately 4.80 ^{o}C higher than the long-term average AWQmiT from 1990 to 2018), average warmest quarterly precipitation (AWQP) was 17.99 mm lower than the long-term AWQP from 1990 to 2018, and average warmest relative humidity quarter (AWRQ) was almost 17% greater than the long-term AWRQ from 1990 to 2018. The average warmest windspeed quarter (AWWQ) was between 23.04 km/h from 2005 to2018, which is 5.30 km/h less than that was during the long term AWWQ from 1990 to 2018 (Table 4). Statistical results of climate factors indicate that daily average warmest quarterly minimum temperature (AWQmiT),

average warmest quarterly maximum temperature (AWQmaT) and average warmest windspeed quarter (AWWQ), mainly affected the time of forest fires in the research area (R^2 = 0.59). However, these were no meaningful correlations between the selected parameters and severity of the fires.

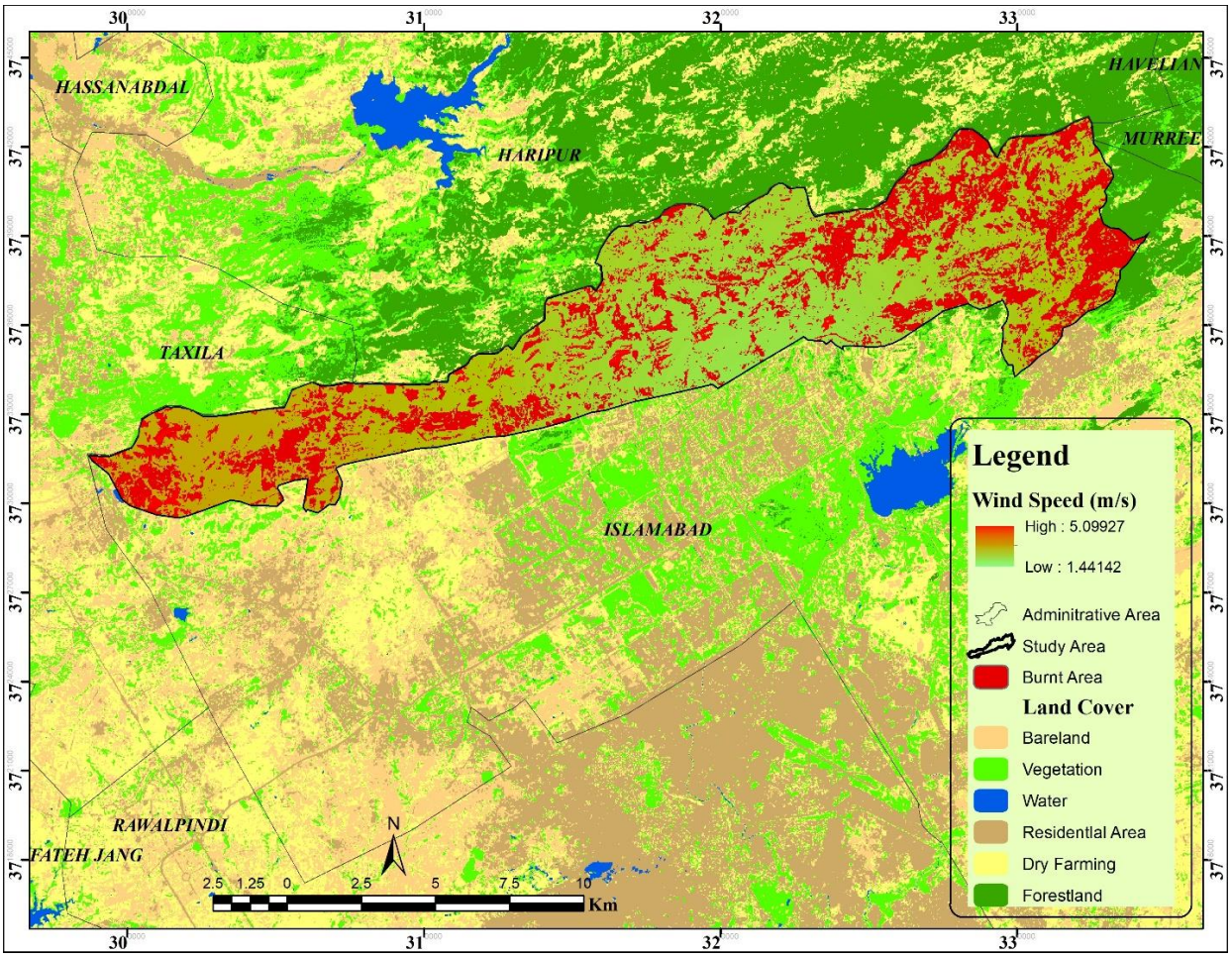

Insert Fig. 4. Spatially overlapping of average warmest windspeed quarter and burnt areas.

Fig. 4 demonstrates that the maximum patches of fire existed in the regions of average warmest windspeed quarter (AWWQ). Furthermore, our analysis indicated that average warmest quarterly minimum temperature (AWQmiT) of P-0.210 and Average warmest quarter maximum temperature (AWQmaT) of P -0.0023 was affected by both the duration of fire and the spread of fire, more by the duration of fire than by the spread of fire in all fire patches (Table 5).

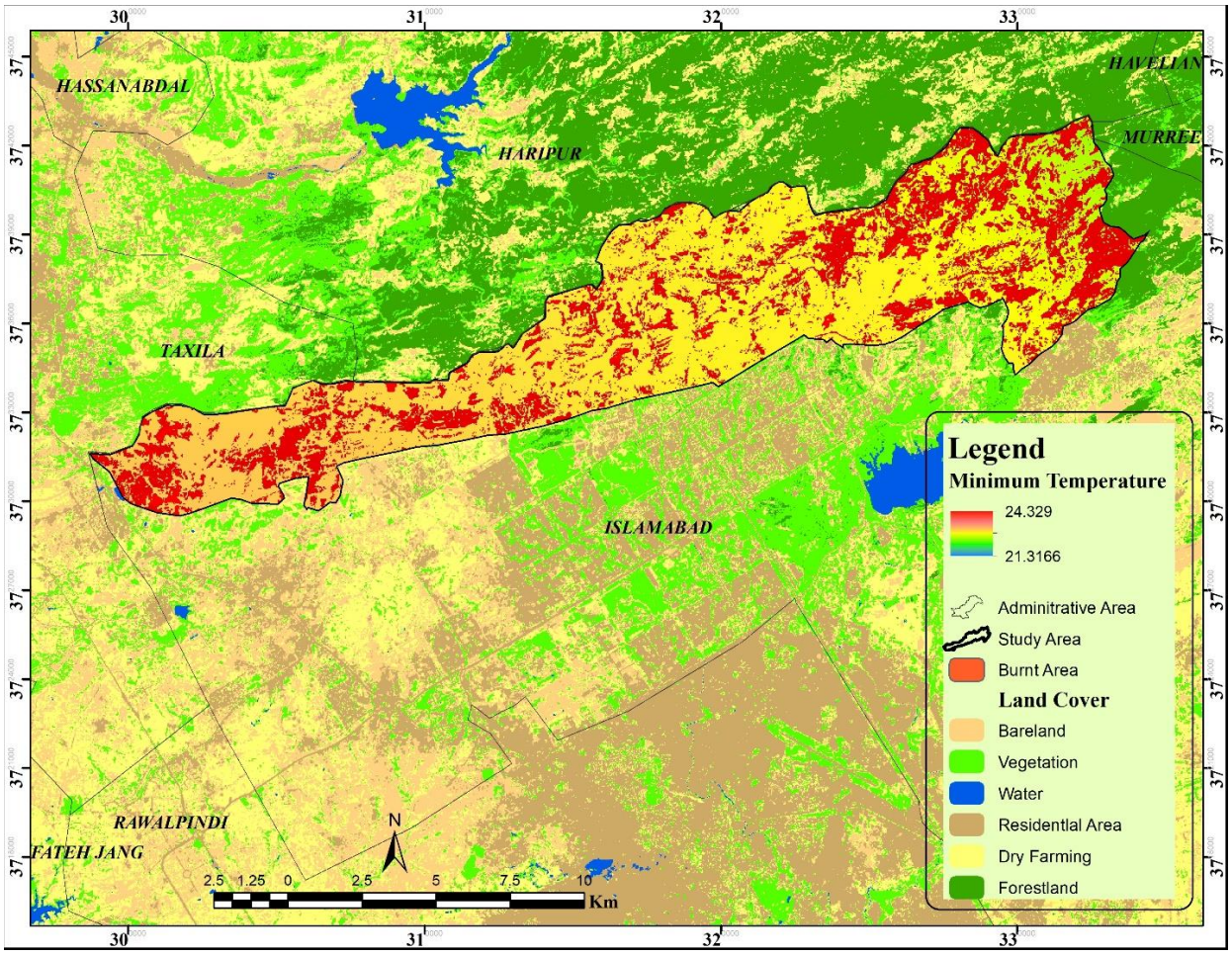

Insert Fig. 5. Spatially overlapping of daily average warmest quarterly minimum temperature (AWQmiT) and burned areas.

Fig. 5 demonstrates that fires at low temperature had no correlation with burned areas. Low temperature did not have a correlation with other parameters.

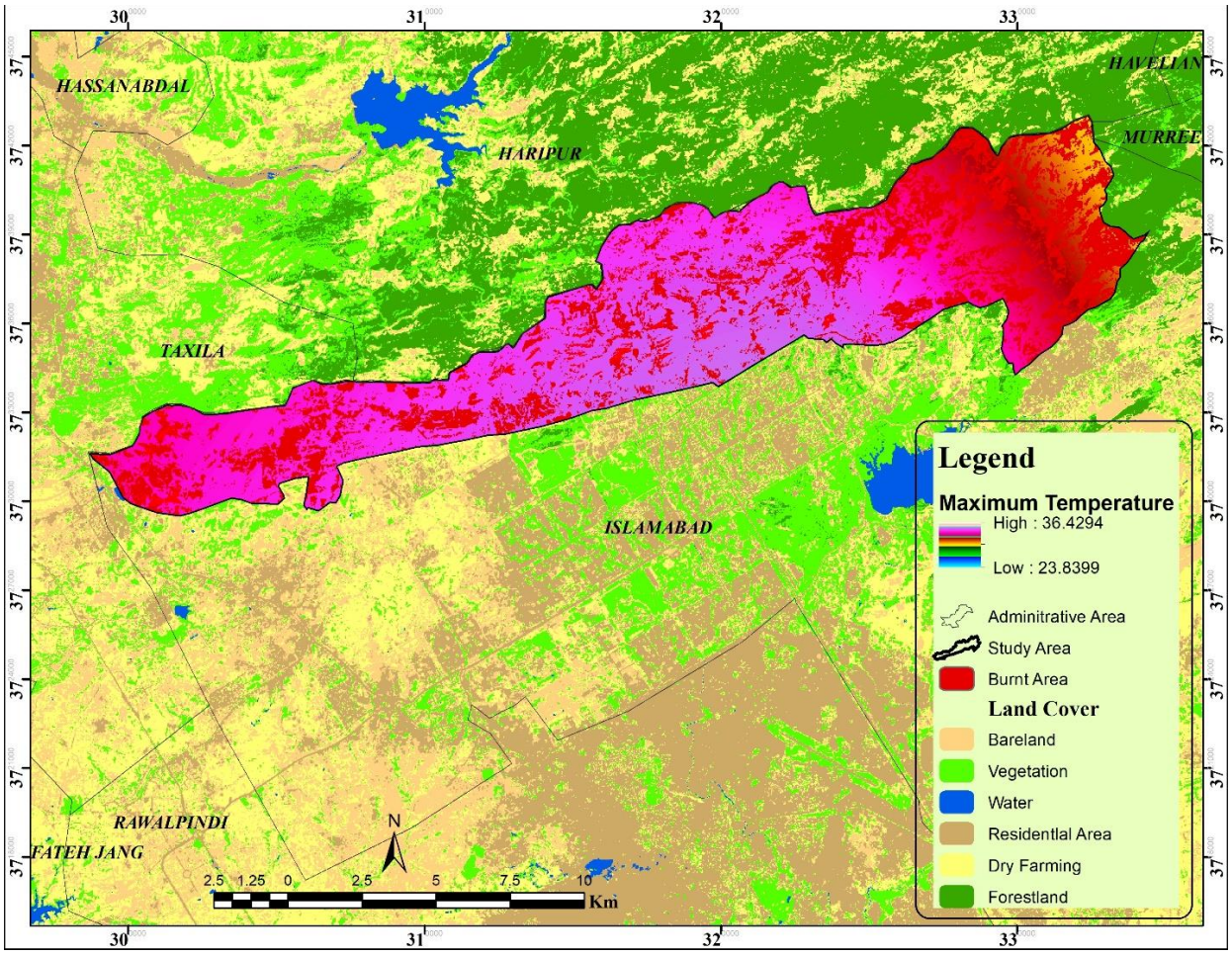

Insert Fig. 6. Spatially overlapping of daily average warmest quarterly maximum temperature (AWQmaT) and burned areas.

Fires occurring at maximum temperatures demonstrated more severe intensity than those occurring at minimum temperatures (Fig. 6). Previous studies have suggested that the environment provides a major influence on the intensity of fire and the fire activity under severe climate change pressure (SCHOENNAGEL et al. 2004; Aldersley et al. 2011; Stan et al. 2014). In this study, average warmest quarterly precipitation, average warmest wind speed quarter and average warmest relative humidity quarter displayed minor variations during wildfires, and no major fire intensity impact. The findings of earlier studies suggest that the risk of forest fire incidence is strongly linked to the annual volume of precipitation (Zhang et al. 2011; Mohammadi et al. 2014). Moreover, only

distance to roads had a strong positive association with longevity of fire across all the variables. The decision coefficient (R^2) for the model to 82.34% as this element was applied to the regression model.

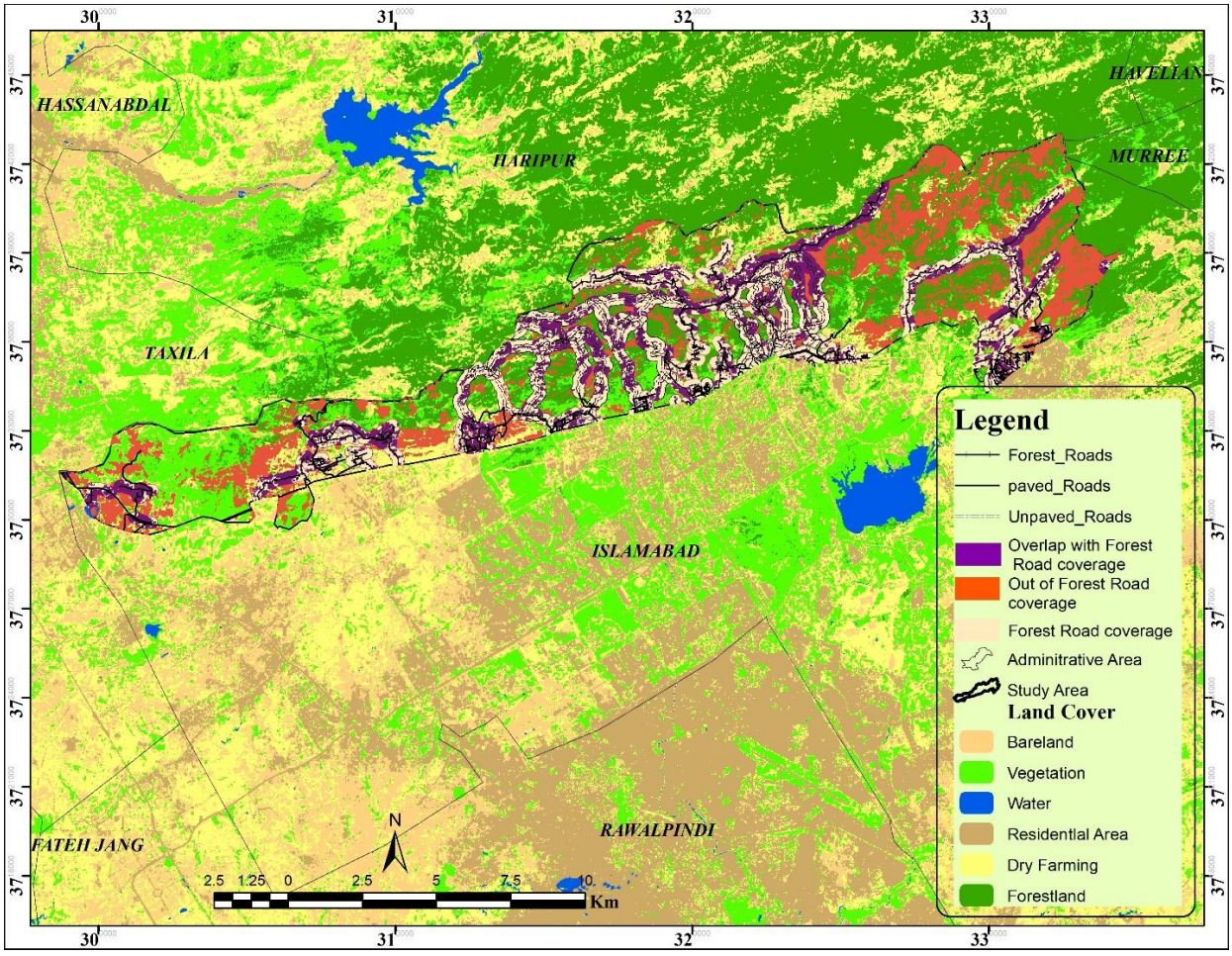

Insert Fig. 7. Burned areas overlapping with and outside of the forest road network.

Fig.7 shows that the forest road network did follow forest road requirements in the study region. The density of road was 3.93 m/ha and coverage of the network of road was detected in 32.97% of the study area. Thus, ideal density of road can decrease the incidence and period of fire, since it is easier to reach fire prone areas. In forest fire studies the proximity to a road is a known key factor (Zhang et al. 2011). An analysis of the destroyed woods found that the bulk of fire spots

were in low road intensity areas. It is, therefore, necessary to find optimum density of road (approximately 20 m/ha) and fair road network coverage (up to 65%) within forest zones (Lotfalian et al. 2016). Access roads enable fire engine movement and reduce the travel time for fire crews to get to forest fires. In such woods, paths may be substituted as main forest roads with low path width. Tracks are also essential for the safety of forest fires because they link to the road network and often serve as a firebreak. They require larger and easier movements to combat a fire within or at the outskirts of a forest (FAO 2009). Certain variables that were anthropogenically mediated showed no major impact on wildfire period (P-0.05). Spatial data (Fig.1) indicates that most wild fires happened in regions with small density of population and at a long distance from public highways. In some cases, average coverage of fire patches is less than 1km from built-up areas and 1.34km from civic highways. Some forest patches are located more than 2 km away from residential areas and approximately 1.5 km away from public highways.

Many parks and hiking trails are present in the study area. Human activities e.g. mining, hiking, farming and timber harvesting could be related to fires. This indicates the need for specific studies into trends, seasonal arrangements and ranges of dissimilar forms of anthropogenic actions in fire sensitive areas. The regression analysis indicates that forest composition has greatly influenced the intensity of fire in terms of environmental variables (Table 4). Forest density not only influenced the fire distribution ($R^2 = 0.82$), but also greatly increased fire patch length (P- 0.001).

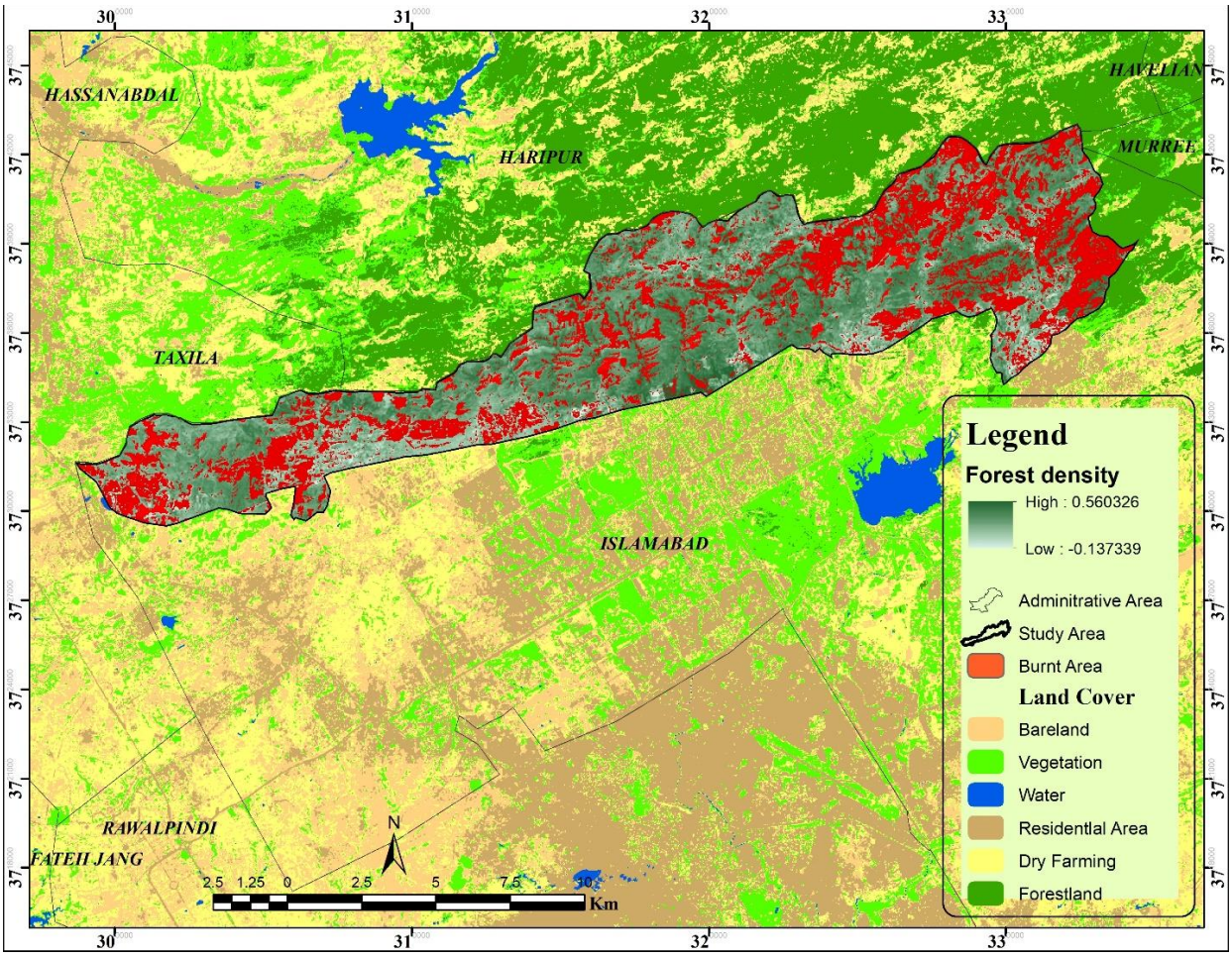

Insert Fig. 8. High NDVI implying the forest density.

The NDVI values range from minimum -0.13 to maximum 0.56 (Fig. 8). The high NDVI values are related to high density of forests. The high-density woods are distinguished by a dense tree crown system, where fire is expected to propagate as an aggressive crown burn, resulting in greater fuel accumulation and therefore increasing the intensity of burning (Duane et al. 2015; Duane 2018). The occurrence of forest fire incidences is high in the dense forest areas of Margalla Hills (Fig. 6). Moreover, in forest systems with high canopy closing, the probability of crown fires is higher due to a rise in vertical and horizontal cohesion (Main and Uhtoff 2002; Lecina-Diaz et al. 2014). Our analysis found no significant association between topographic parameters (aspect, slope, TPI, TWI and plan curvature) and fire intensity (P-0.06). Nevertheless, most fires happened

in the eastern and southwestern parts. Nearly 52% of the fire prone areas are located in the eastern part, as this area received more solar radiation and less humidity (Alexander et al. 2006). The average slope in the burned patches was less steep and estimated approximately 44%, Various studies have found that as the slope increase , the gap and angle between fire and materials reduces which contributes to more severe intensity of fires (Finney and McAllister 2011; Lecina-Diaz et al. 2014; Werth et al. 2016). However, in our study area slope has not shown any major impact on the intensity of the fire.

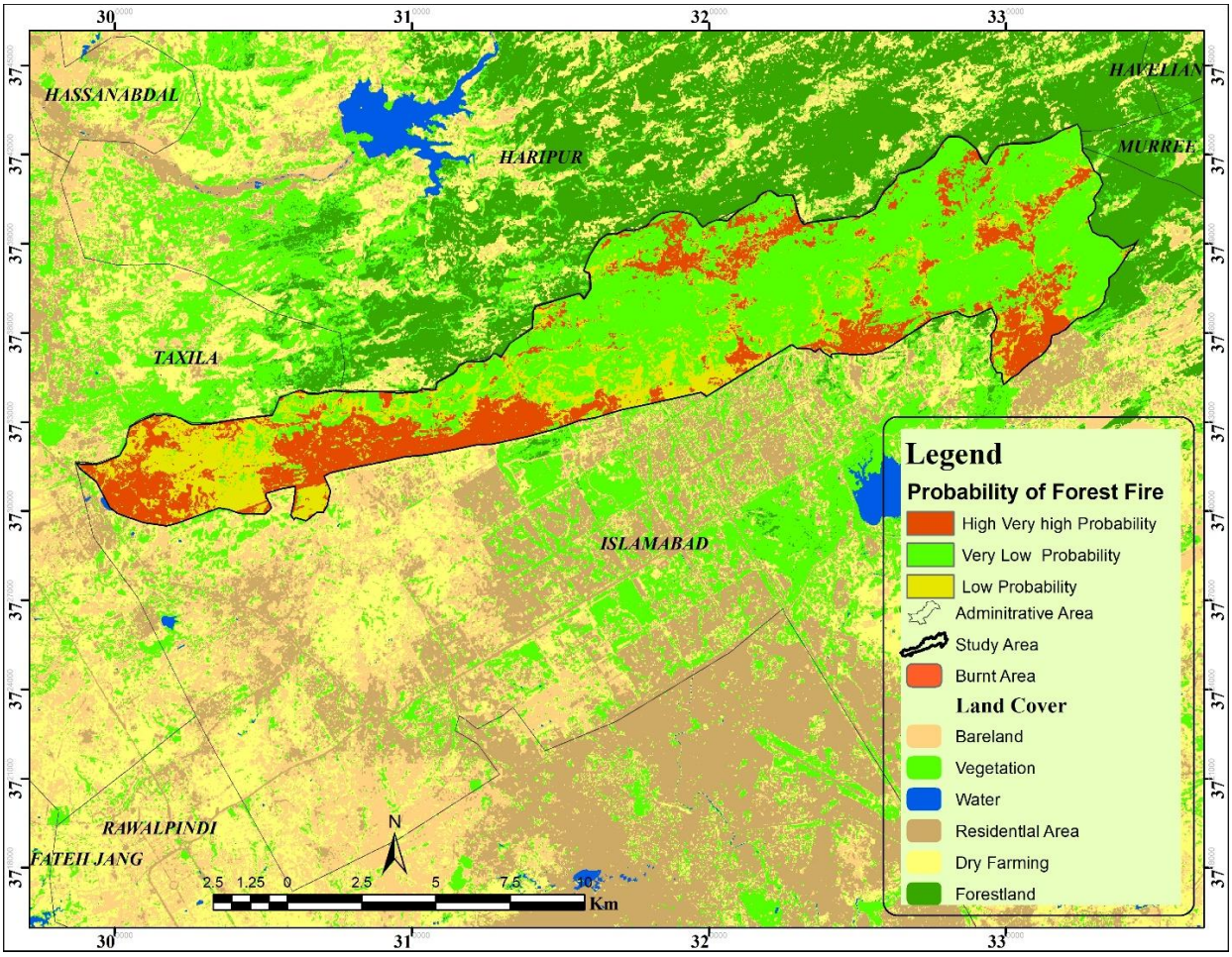

Insert Fig. 9. Susceptibility map of spreading forest fires dependent on duration/time.

Fig. 9 illustrate that risk analysis of forest fire using critical fire resilience criteria classifies three threat levels by intensity. According to the analysis 22% of forests are located in the high and very high-risk level (> 0.65), 25% are in the low risk level (0.45-0.65), and 53% are in the very low risk severity level (0.25 – 0.45). Table 4 indicates that the path to the forest road was the best predictor with a determination coefficient of 72.64% affecting the length of the forest fire. Our results indicate that in all the woods, average road density was around 3.23 m/ha, although in the fire areas this number was somewhat smaller, 2.14 m/ha (Fig. 7).

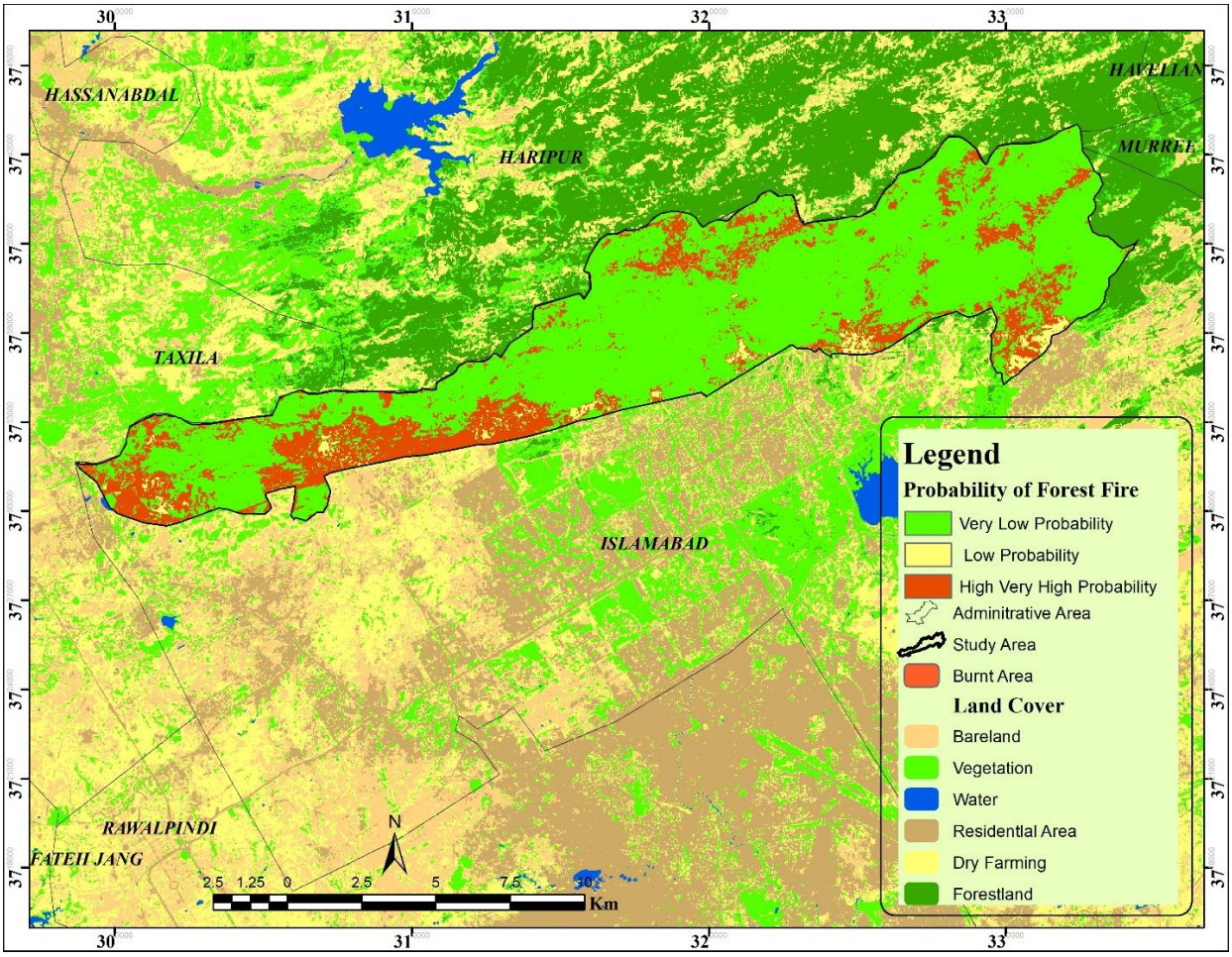

Insert Fig. 10. Susceptibility map of spreading forest fires.

Road density in the study region is far from the appropriate requirements, i.e. 20 m/ha. Due to length of the fires, nearly 2/3 of the research region is in the medium and above threat range and it is impossible to establish a forest road network of acceptable capacity and good coverage. Moreover, the results of the fire spread probability map showed that the vast majority (80%) of forests are situated at very low severity (69%), low severity (6%) and high and very high severity level (5%) (Fig. 10). Larger forest patches with longer burn periods seemed to locate in the remote extents of low road coverage that were situated mainly at higher elevations. Therefore, less road lines increase fuel cohesion and result in a less fractured region. As an outcome, bigger and lengthier fires occurred, especially in areas of minor road density and timid road network cover. Additionally, in ground-based activities, greater fires appeared in remote areas with limited visibility for firefighting teams. (Pew and Larsen 2001; Holsinger et al. 2016). Lower road densities render it safer for the fire departments to reach gear and function as firebreaks in fire suppression (Narayanaraj and Wimberly 2012; Ricotta et al. 2018). The major influencing factor in human-induced fires is the distance to the forest route. Greater road masses represent a greater degree of human operations and disturbances (Syphard et al. 2007, 2011; Yap 2018). Their analysis offers innovative data on the correlation of climatic, vegetation, topography, and human activities in the Margalla Hills and on the resilience of fire and fire spread over a brief period. While the intensity of fire is affected by environmental factors and high density of forest, roads of forest are the single biggest manipulating restriction for extending the time of a fire, mainly in complex elevated woods, comparatively lower density of road and lower road network cover.

4 Conclusion

Wildfires pose a significant danger to the Margalla Hills forests, Islamabad, Pakistan. Forest-fires are major contemporary challenge to forest resources conservation in Margalla, Islamabad. Almost

25812.36 ha forest area was burned from May 2005 to July 2018. The burned area was estimated using Landsat data and validated with field data. The scale of the fire patches was estimated as 0.3 to 2523 hectares. Our findings show that with increasing cumulative days after the start of forest fire the burned areas have increased in the months of May, June and July (2005 to 2018) at a pace of 25.848 ha /day. Average burned area was 1707.3 ha/year, that eventually increase burning around 7% of the overall forested region in less than a month. We investigated the variables affecting the length of these wildfires and their distribution. Forest density had a major effect on the length and distribution of wildfires among the parameters of the study. While topographical factors (TPI, slope, aspect, TWI, and curvature of the plane) hardly take effect. Through spatial analysis, it is found that in certain areas with extensive forest coverage, such as the southwestern and eastern sections of our study location, major fires happened. We also observed an interesting association between fire intensity (fire spread and duration/time) and mean temperature, although wind direction only affected the length of fire substantially. During a forest-fire, there were no important differences between the intensity of the fire and other environmental conditions (mean precipitation and humidity). Many forests in Pakistan have a low forest road network and therefore, it is difficult to reach the whole forest area. Spatial analyses found that most wildfires happened in less populated areas and at a long distance from public roads, but some anthropogenic behaviors could have influenced fire growth.

In practice, RS and GIS is a useful technique for exploring forest fire and their distribution. By using various meteorological models to evaluate the impact of weather on forest region and the influence of urban heat island in Islamabad, this work can be further elaborated.

Availability of data and material

The datasets generated and/or analyzed during the current study are not publicly available but are available from the corresponding author on reasonable request.

Competing interests

The author declares that there is no conflict of interest in this manuscript's publication. Moreover, the writers have thoroughly addressed ethical issues, including plagiarism, informed consent, fraud, data manufacturing and/or falsification, dual publication and/or submission and redundancy.

Funding

This work is supported jointly by the National Key Research Development Program of China (No. 2017YFB0503604 and No. 2016YFB0502204), National Natural Science Foundation of China (No.61971316) and State Key Laboratory of Satellite Navigation System and Equipment Technology.

Acknowledgements

We would like to pay special and heart whelming thanks to USGS (Earth explorer) department for providing us Landsat 7 (ETM+) and 8 (OLI/TIRS) data and Capital Development Authority (CDA), Islamabad, Pakistan for digital and all ancillary data. We are also thankful to Dr. Shazada Adnan, Pakistan Meteorological Department, Islamabad, Pakistan; they are providing all meteorological data related with this research. We also admire Dr. Muhammad Imran of Institute of Geoinformation and earth observation (IGEO), University of Arid Agriculture, Rawalpindi for their facilitation at various stages of the field campaign. We are highly regarding the unspecified reviewers and editors of journal for providing helpful inputs that improved the manuscript.

Contributions

AT plan conceptualization, methodology, systematic review, testing, examination, tools, and curation of data and preparation of initial draft. HS all work is reviewed, compiled, and supervised. SS reviewed all manuscript and add compiled final manuscript.

References

Abdi O, Kamkar B, Shirvani Z, et al (2018) Spatial-statistical analysis of factors determining forest fires: A case study from Golestan, Northeast Iran. Geomatics, Nat Hazards Risk 9:267–280. https://doi.org/10.1080/19475705.2016.1206629

Abdi O, Universit T, Shirvani Z, Universit T (2016) The impact of forest management on forest fires in 2010 of Golestan Province by using GIS. 1–2

Aldersley A, Murray SJ, Cornell SE (2011) Global and regional analysis of climate and human drivers of wildfire. Sci Total Environ 409:3472–3481. https://doi.org/10.1016/j.scitotenv.2011.05.032

Alexander JD, Seavy NE, Ralph CJ, Hogoboom B (2006) Vegetation and topographical correlates of fire severity from two fires in the Klamath-Siskiyou region of Oregon and California. Int J Wildl Fire 15:237–245. https://doi.org/10.1071/WF05053

Bhunia GS, Dikhit MR, Kesari S, et al (2011) Role of remote sensing, geographic bioinformatics system and bioinformatics in kala-azar epidemiology. J Biomed Res 25:373–384. https://doi.org/10.1016/S1674-8301(11)60050-X

Blocks M and MN (2007) Environmental Baseline study. 146

Bonazountas M, Kallidromitou D, Kassomenos P, Passas N (2007) A decision support system for managing forest fire casualties. J Environ Manage 84:412—418. https://doi.org/10.1016/j.jenvman.2006.06.016

Brooks M, Lusk M (2008) Fire Management and Invasive Plants

Calkin DE, Cohen JD, Finney MA, Thompson MP (2014) How risk management can prevent future wildfire disasters in the wildland-urban interface. Proc Natl Acad Sci U S A 111:746–751. https://doi.org/10.1073/pnas.1315088111

Collen B, Kock R, Heinrich M, et al (2015) Biodiversity and ecosystems

Cortez P (2006) A Data Mining Approach to Predict Forest Fires using Meteorological Data

Cutler R, Lawler J, Thomas Edwards J, et al (2007) Random Forests for Classification in Ecology. Ecology 88(11):2783–2792

Department BIF (1927) The forest act, 1927

Duane A (2018) Assessing global change impacts on fire regimes in Mediterranean ecosystems

Duane A, Brotons L (2018) Synoptic weather conditions and changing fire regimes in a

494 Mediterranean environment. Agric For Meteorol 253–254:190–202.
495 https://doi.org/10.1016/j.agrformet.2018.02.014

496 Duane A, Piqué M, Castellnou M, Brotons L (2015) Predictive modelling of fire occurrences
497 from different fire spread patterns in Mediterranean landscapes. Int J Wildl Fire 24:407–418

498 Escuin S, Navarro R, Fernández P (2008) Fire severity assessment by using NBR (Normalized
499 Burn Ratio) and NDVI (Normalized Difference Vegetation Index) derived from LANDSAT
500 TM/ETM images. Int J Remote Sens 29:1053–1073.
501 https://doi.org/10.1080/01431160701281072

502 FAO (2009) International Handbook on Forest Fire Protection - Technical guide for the countries
503 of the Mediterranean basin. 1–163

504 Finney MA, McAllister SS (2011) A review of fire interactions and mass fires. J Combust 2011:.
505 https://doi.org/10.1155/2011/548328

506 Fusco E, Bradley B, Abatzoglou JT (2018) Human-Related Ignitions Increase the Number of
507 Large Wildfires across U.S. Ecoregions. Fire 1:4. https://doi.org/10.3390/fire1010004

508 Holsinger L, Parks SA, Miller C (2016) Weather, fuels, and topography impede wildland fire
509 spread in western US landscapes. For Ecol Manage 380:59–69.
510 https://doi.org/10.1016/j.foreco.2016.08.035

511 Iqbal MF, Riaz Khan M, Malik AH (2013) Land use change detection in the limestone
512 exploitation area of Margalla Hills National Park (MHNP), Islamabad, Pakistan using geo-
513 spatial techniques. J Himal Earth Sci 46:89–98

514 Islamabad CC (2015) Year book 2015-16

515 Jensen JR, Lulla K (1987) Introductory digital image processing: A remote sensing perspective.
516 Geocarto Int 2:65. https://doi.org/10.1080/10106048709354084

517 Khalid N, Saeed Ahmad S (2015) Monitoring Forest Cover Change of Margalla Hills Over a
518 Period of Two Decades (1992-2011): A Spatiotemporal Perspective. J Ecosyst Ecography
519 06:1–8. https://doi.org/10.4172/2157-7625.1000174

520 Krebs P, Pezzatti GB, Mazzoleni S, et al (2010) Fire regime: History and definition of a key
521 concept in disturbance ecology. Theory Biosci 129:53–69. https://doi.org/10.1007/s12064-
522 010-0082-z

523 Lecina-Diaz J, Alvarez A, Retana J (2014) Extreme fire severity patterns in topographic,
524 convective and wind-driven historical wildfires of Mediterranean pine forests. PLoS One
525 9:e85127. https://doi.org/10.1371/journal.pone.0085127

526 Lesmeister DB, Sovern SG, Davis RJ, et al (2019) Mixed-severity wildfire and habitat of an old-
527 forest obligate. Ecosphere 10:. https://doi.org/10.1002/ecs2.2696

528 Lotfalian M, Khosrozadeh S, Hosseini SA, et al (2016) Determination of forest skid trail density
529 in Caspian forests, Iran. J For Sci 62:80–87. https://doi.org/10.17221/84/2015-JFS

530 Main M, Uhtoff P (2002) The Ashland Wildland/Urban Interface Wildfire Management
531 Inventory, Analysis, and Opportunities

Masek JG, Vermote EF, Saleous NE, et al (2006) A landsat surface reflectance dataset for North America, 1990-2000. IEEE Geosci Remote Sens Lett 3:68–72. https://doi.org/10.1109/LGRS.2005.857030

Mohammadi F, Bavaghar MP, Shabanian N (2014) Forest Fire Risk Zone Modeling Using Logistic Regression and GIS: An Iranian Case Study. Small-scale For 13:117–125. https://doi.org/10.1007/s11842-013-9244-4

Muhammad Ibrar Shinwari, . MAK (2000) Vegetation Comparison of Sacred, Reserved and Unreserved Sites of Rumli Village at Margalla Hills National Park, Islamabad. Pakistan J Biol Sci 3:1681–1683. https://doi.org/10.3923/pjbs.2000.1681.1683

Mulder VL, de Bruin S, Schaepman ME, Mayr TR (2011) The use of remote sensing in soil and terrain mapping - A review. Geoderma 162:1–19

Narayanaraj G, Wimberly MC (2012) Influences of forest roads on the spatial patterns of human- and lightning-caused wildfire ignitions. Appl Geogr 32:878–888. https://doi.org/10.1016/j.apgeog.2011.09.004

Oliveira S, Oehler F, San-Miguel-Ayanz J, et al (2012) Modeling spatial patterns of fire occurrence in Mediterranean Europe using Multiple Regression and Random Forest. For Ecol Manage 275:117–129. https://doi.org/10.1016/j.foreco.2012.03.003

Ouaidrari H, Vermote EF (1999) Operational Atmospheric Correction of Landsat TM Data based on a simplified formulation of the signal in order. Remote Sens Environ 15:4–15. https://doi.org/10.1016/S0034-4257(99)00054-1

Parks SA, Parisien MA, Miller C (2011) Multi-scale evaluation of the environmental controls on burn probability in a southern Sierra Nevada landscape. Int J Wildl Fire 20:815–828. https://doi.org/10.1071/WF10051

Pew KL, Larsen CPS (2001) GIS analysis of spatial and temporal patterns of human-caused wildfires in the temperate rain forest of Vancouver Island, Canada. For Ecol Manage 140:1–18. https://doi.org/10.1016/S0378-1127(00)00271-1

Ricotta C, Bajocco S, Guglietta D, Conedera M (2018) Assessing the Influence of Roads on Fire Ignition: Does Land Cover Matter? Fire 1:24. https://doi.org/10.3390/fire1020024

Roy DP, Kovalskyy V, Zhang HK, et al (2016) Characterization of Landsat-7 to Landsat-8 reflective wavelength and normalized difference vegetation index continuity. Remote Sens Environ 185:57–70. https://doi.org/10.1016/j.rse.2015.12.024

Roy DP, Wulder MA, Loveland TR, et al (2014) Landsat-8: Science and product vision for terrestrial global change research. Remote Sens Environ 145:154–172. https://doi.org/10.1016/j.rse.2014.02.001

Rtificial ANA, Pproach INA (2015) P REDICTING B URNED A REAS OF F OREST F IRES : Fire Ecol 11:106–118. https://doi.org/10.4996/fireecology.110106

Samanta S, Pal DK, Lohar D, Pal B (2011) Modeling of temperature and rainfall of West Bengal through remote sensing and GIS techniques. Int J Geoinformatics 7:31–40

570 Schoennagel T, Veblen TT, Romme WH (2004) The interaction of fire, fuels, and climate across
571 Rocky Mountain forests. Bioscience 54:661–676

572 SCHOENNAGEL T, VEBLEN TT, ROMME WH (2004) The Interaction of Fire, Fuels, and
573 Climate across Rocky Mountain Forests. Bioscience 54:661. https://doi.org/10.1641/0006-
574 3568(2004)054[0661:tioffa]2.0.co;2

575 Skakun S, Li Z, Roger J, et al (2018) Characterization of Sentinel-2A and Landsat-8 top of
576 atmosphere, surface, and nadir BRDF adjusted reflectance and NDVI differences. Remote
577 Sens. Environ. 215:482–494

578 Stan AB, Fulé PZ, Ireland KB, Sanderlin JS (2014) Modern fire regime resembles historical fire
579 regime in a ponderosa pine forest on Native American lands. Int J Wildl Fire 23:686–697.
580 https://doi.org/10.1071/WF13089

581 Storey J, Choate M, Lee K (2014) Landsat 8 operational land imager on-orbit geometric
582 calibration and performance. Remote Sens 6:11127–11152.
583 https://doi.org/10.3390/rs61111127

584 Syeda Ifrah Ali Abidi and Junaid Noor (2013) Economic Analysis of Forest Management in
585 Pakistan - A Case Study of Changa Mange and Muree Forest. Munich Pers RePEc Arch

586 Syphard AD, Keeley JE, Brennan TJ (2011) Comparing the role of fuel breaks across southern
587 California national forests. For Ecol Manage 261:2038–2048.
588 https://doi.org/10.1016/j.foreco.2011.02.030

589 Syphard AD, Radeloff VC, Keeley JE, et al (2007) Human influence on California fire regimes.
590 Ecol Appl 17:1388–1402. https://doi.org/10.1890/06-1128.1

591 Tanvir MS, Mujtaba IM (2006) Neural network based correlations for estimating temperature
592 elevation for seawater in MSF desalination process. Desalination 195:251–272.
593 https://doi.org/10.1016/j.desal.2005.11.013

594 V. Radha Krishna Murthy (2004) Crop Growth Modeling and Its Applications in Agricultural
595 Meteorology. Satell Remote Sens GIS Appl Agric Meteorol 235

596 Valdez MC, Chang KT, Chen CF, et al (2017) Modelling the spatial variability of wildfire
597 susceptibility in Honduras using remote sensing and geographical information systems.
598 Geomatics, Nat Hazards Risk 8:876–892. https://doi.org/10.1080/19475705.2016.1278404

599 Veraverbeke S, Lhermitte S, Verstraeten WW, Goossens R (2010) The temporal dimension of
600 differenced Normalized Burn Ratio (dNBR) fire/burn severity studies: the case of the large
601 2007 Peloponnese wildfires in Greece. Remote Sens Environ 114:2548–2563

602 Viegas DX, Bovio G, Ferreira A, et al (1999) Comparative study of various methods of fire
603 danger evaluation in southern Europe. Int J Wildl Fire 9:235.
604 https://doi.org/10.1071/wf00015

605 Werth PA, Potter BE, Alexander ME, et al (2016) Synthesis of knowledge of extreme fire
606 behavior: Volume 2 for Fire Behavior Specialists, Researchers, and Meteorologists. Gen
607 Tech Rep PNW-GTR-891 2:258

Yap TA (2018) Re: Wildfire Impacts to Poorly-planned Development in San Diego County

Zhang JH, Yao FM, Liu C, et al (2011) Detection, emission estimation and risk prediction of forest fires in China using satellite sensors and simulation models in the past three decades-An overview. Int J Environ Res Public Health 8:3156–3178. https://doi.org/10.3390/ijerph8083156

(1994) Pakistan Protected Areas M e e t i n g

Abbreviations

CDA: Capital Development Authority

NDVI: Normalized Differentiate Vegetation Index

NBR: Normalized Burn Ratio

dNBR: Differentiate Normalized Burn Ratio

RS: Remote Sensing

GIS: Geographic Information System

DEM: Digital Elevation Model SAR: Synthetic-Aperture-Radar

TPI: Terrain Position Index

TWI: Topographic Wetness Index

DTM: Digital Terrain Model

KPK: Khyber Pakhtun Khwa

PMD: Pakistan Meteorological Department

UTM: Universal-Transverse-Mercator

TOA: Top-Of-Atmosphere

USGS: United States Geological Survey

ETM +: Enhanced Thematic Mapper Plus

OLI: Operational Land Imager

DN: Digital Number

Figures

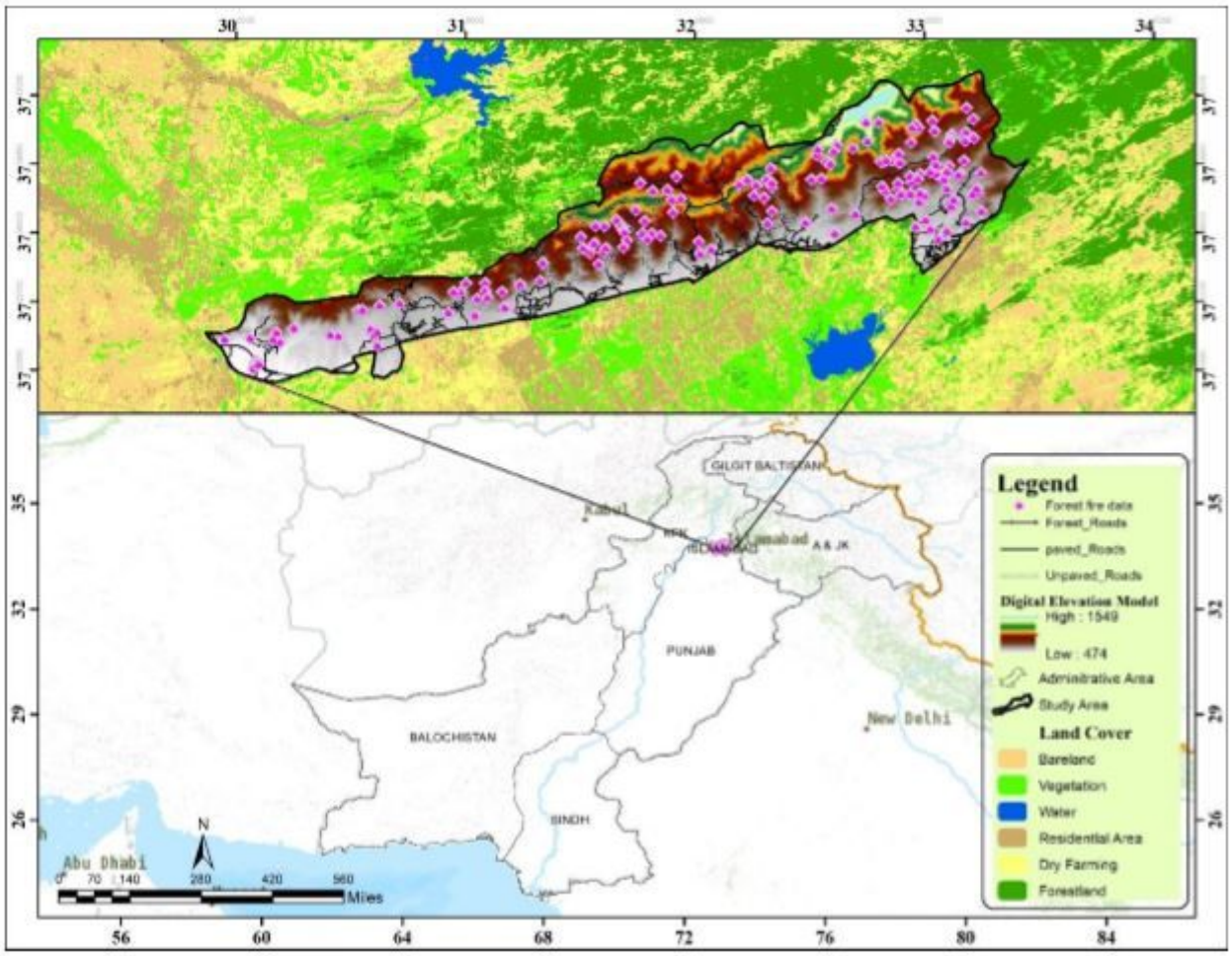

Figure 1

Geographical location of study area, red points referring to the spatial distribution of most forest fire occurrence area.

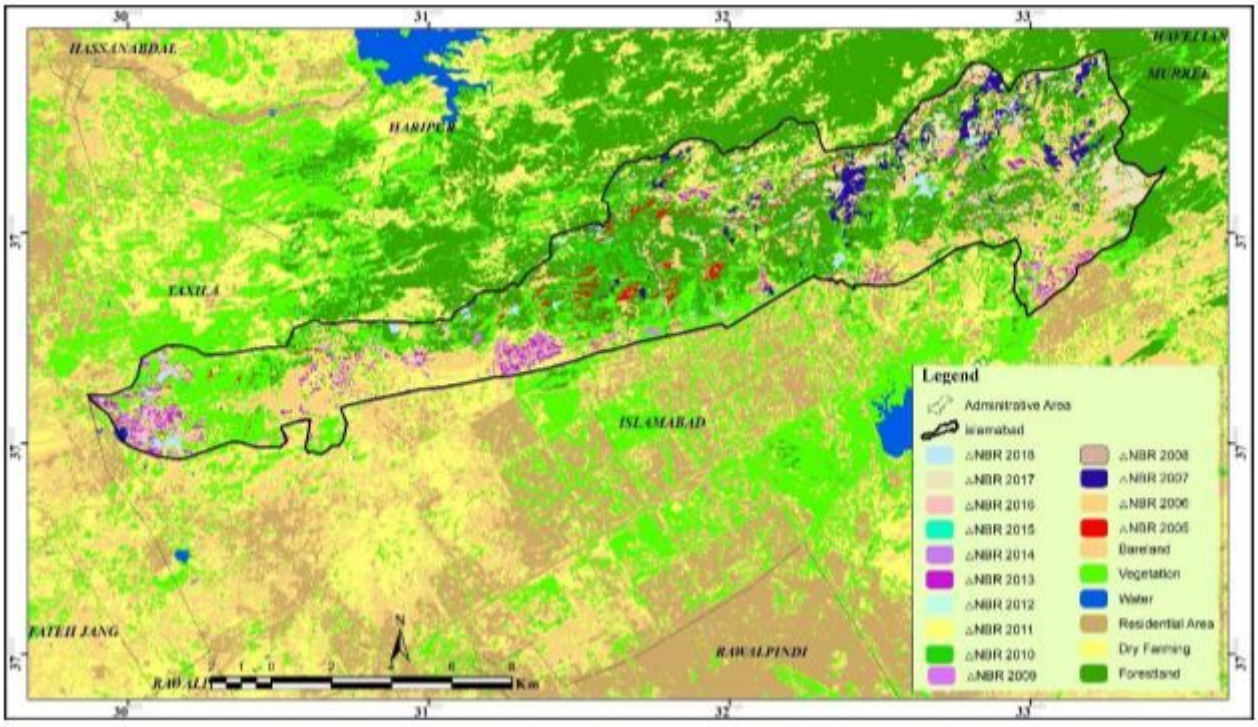

Figure 2

Delta normalized burn ratio map of Margalla hills varying annually.

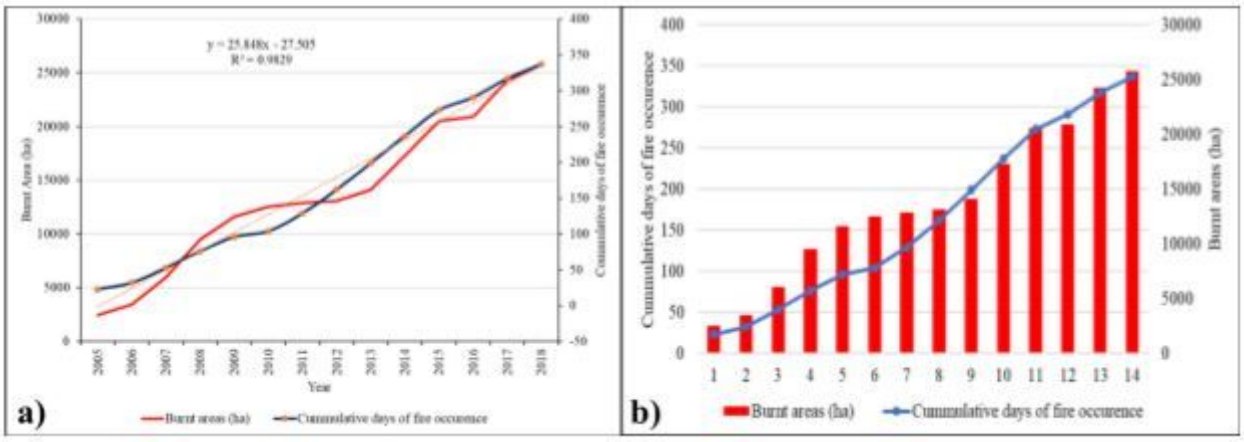

Figure 3

a) Logistic regression comparison between burnt area and fire duration in the experimental region and b) Total days of incidence of fire against burnt region (total cumulative days).

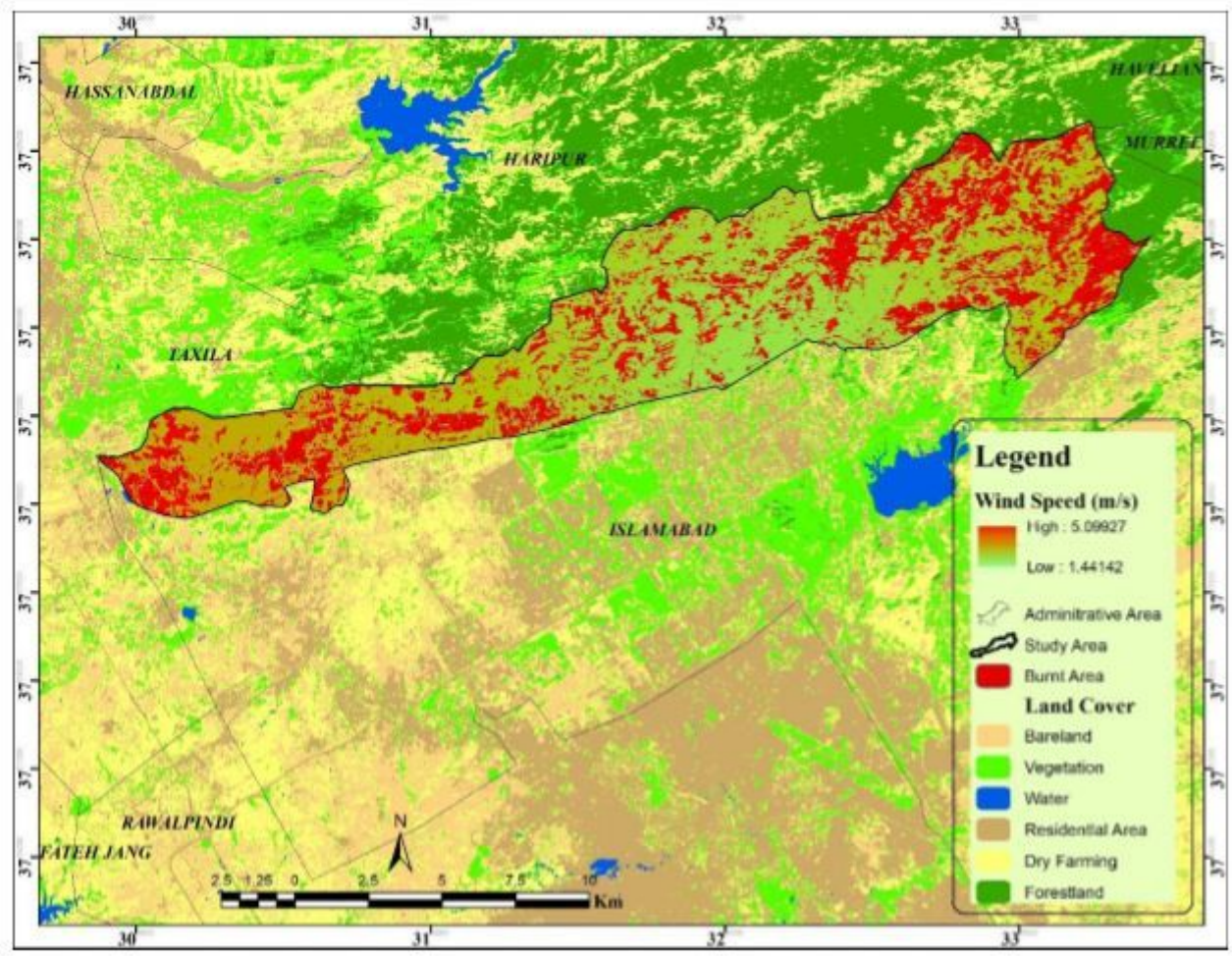

Figure 4

Spatially overlapping of average warmest windspeed quarter and burnt areas.

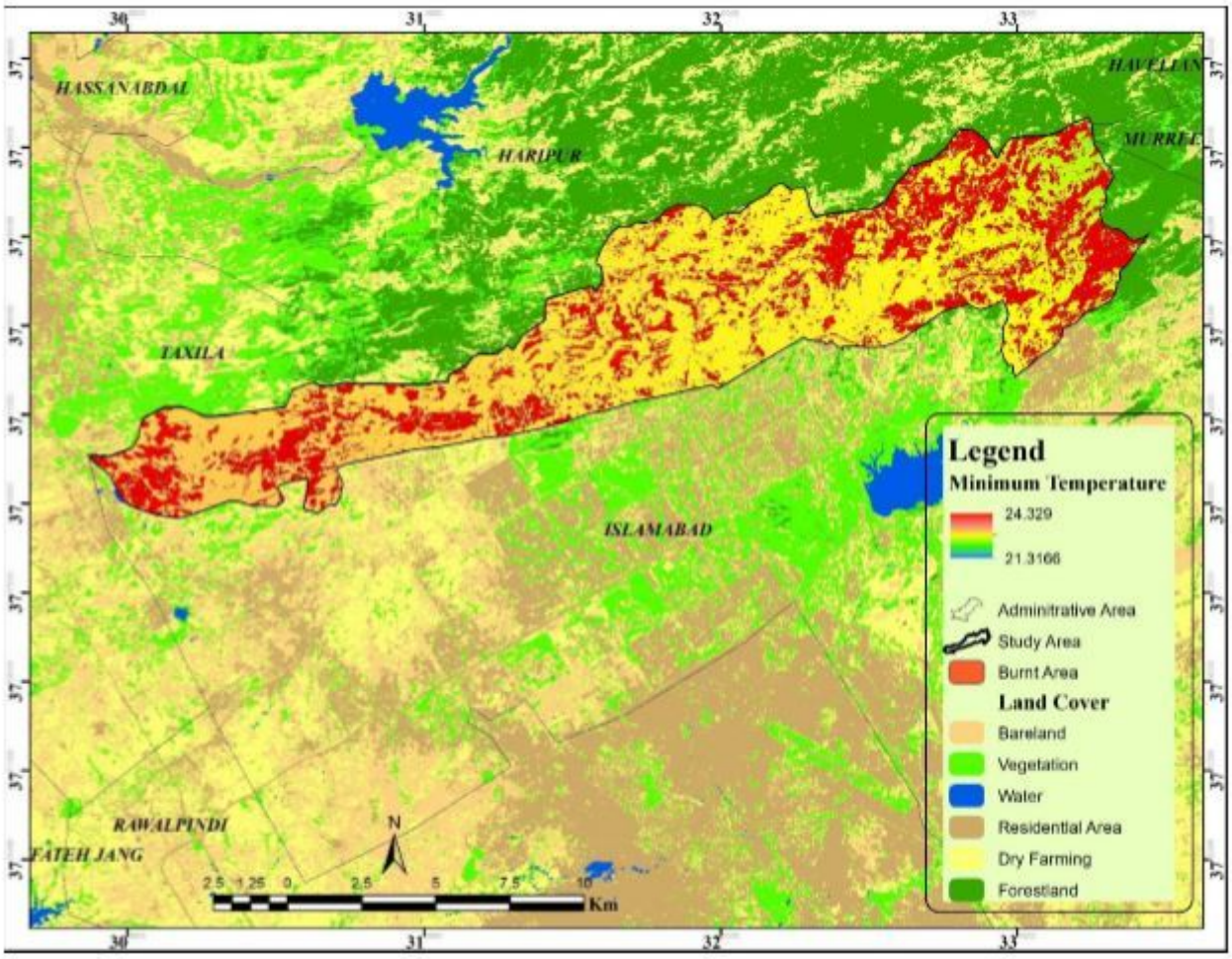

Figure 5

Spatially overlapping of daily average warmest quarterly minimum temperature (AWQmiT) and burned areas.

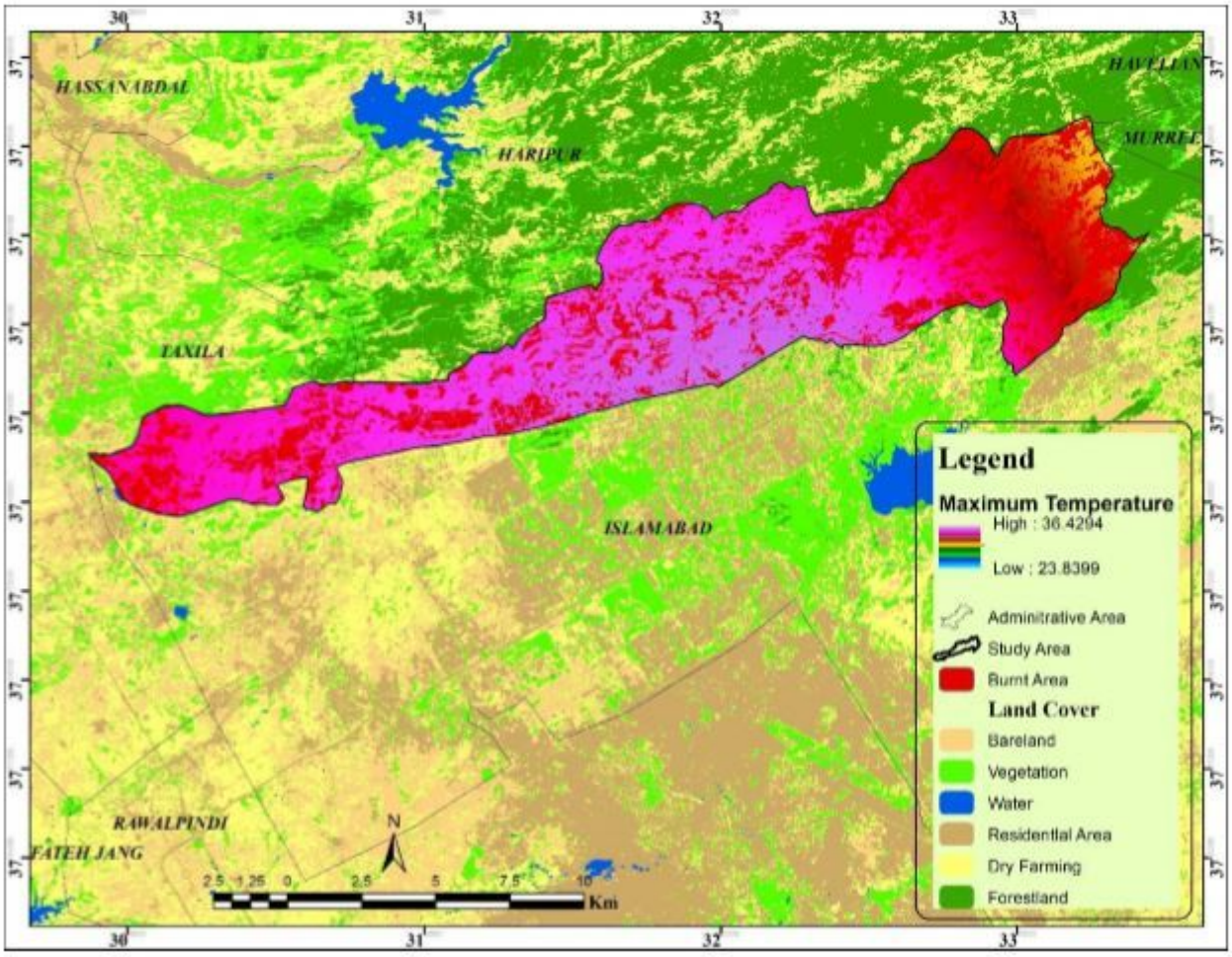

Figure 6

Spatially overlapping of daily average warmest quarterly maximum temperature (AWQmaT) and burned areas.

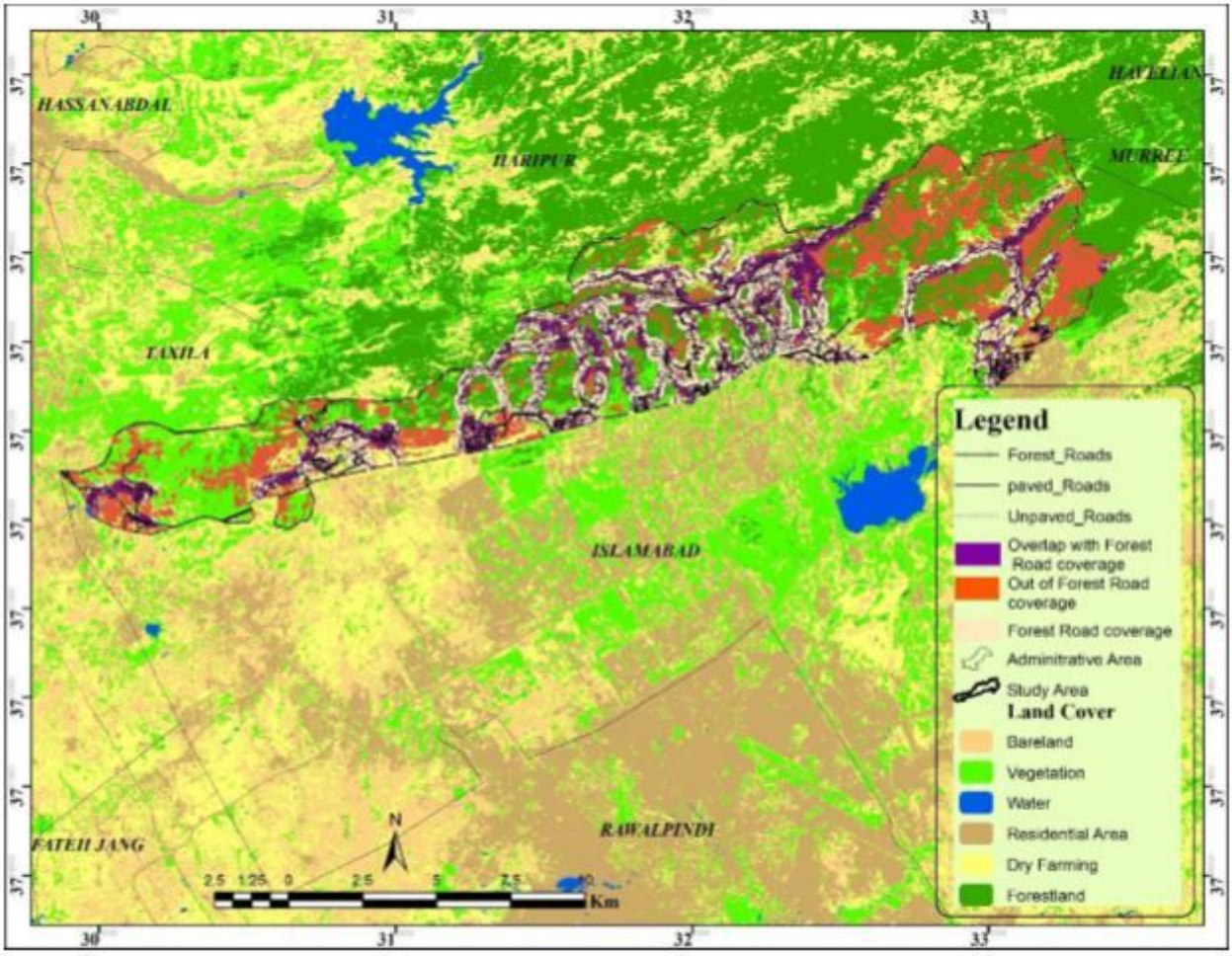

Figure 7

Burned areas overlapping with and outside of the forest road network.

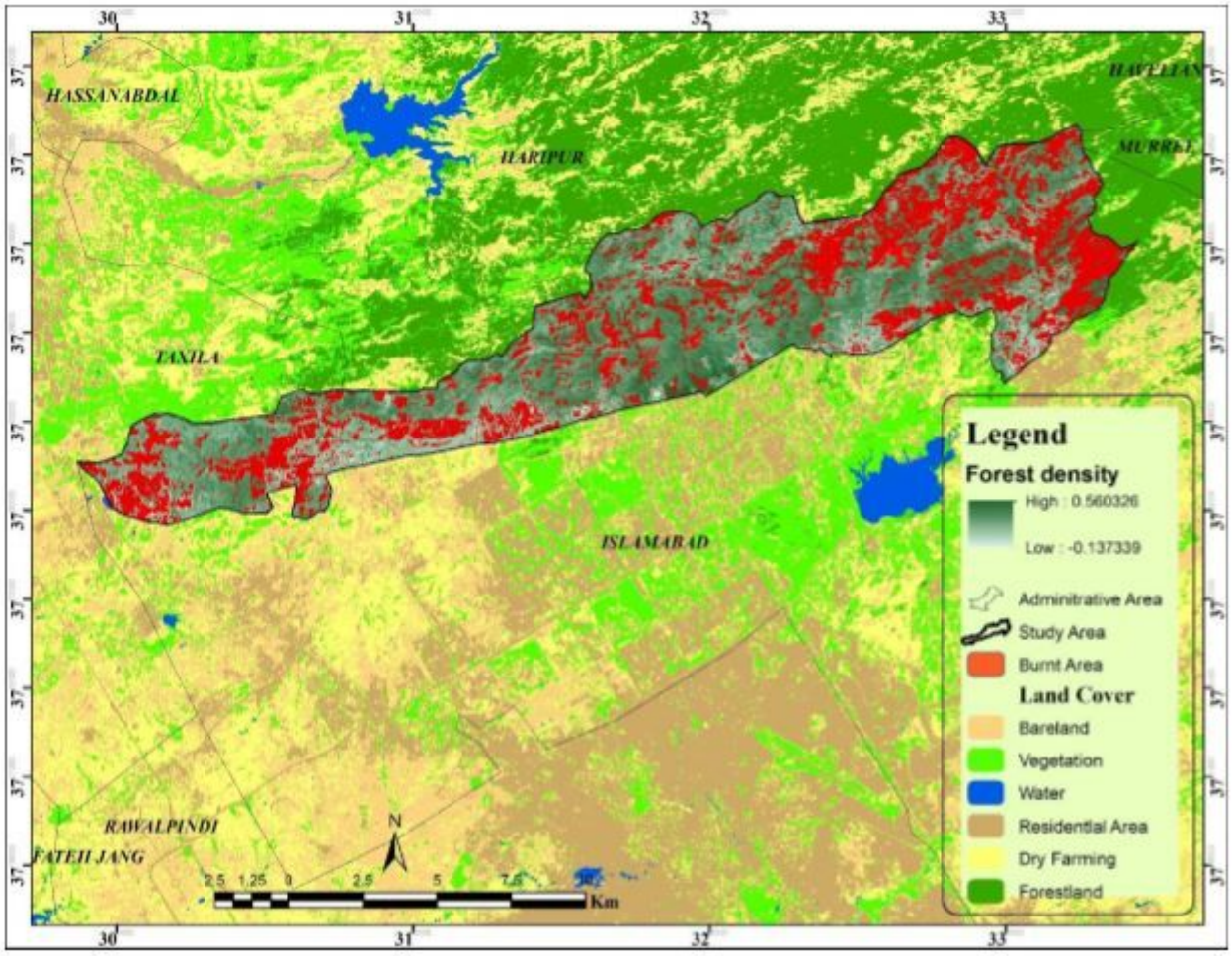

Figure 8

High NDVI implying the forest density.

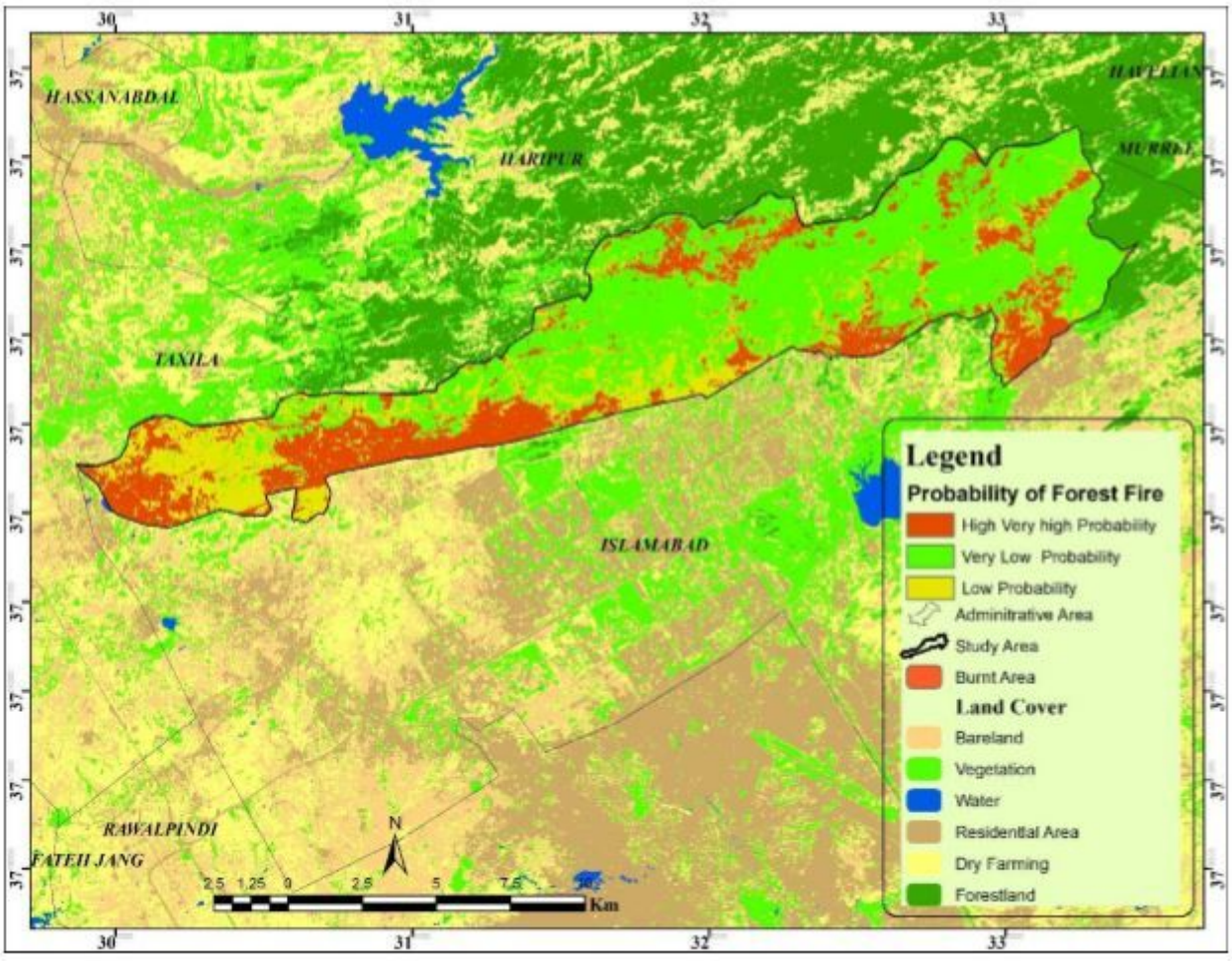

Figure 9

Susceptibility map of spreading forest fires dependent on duration/time.

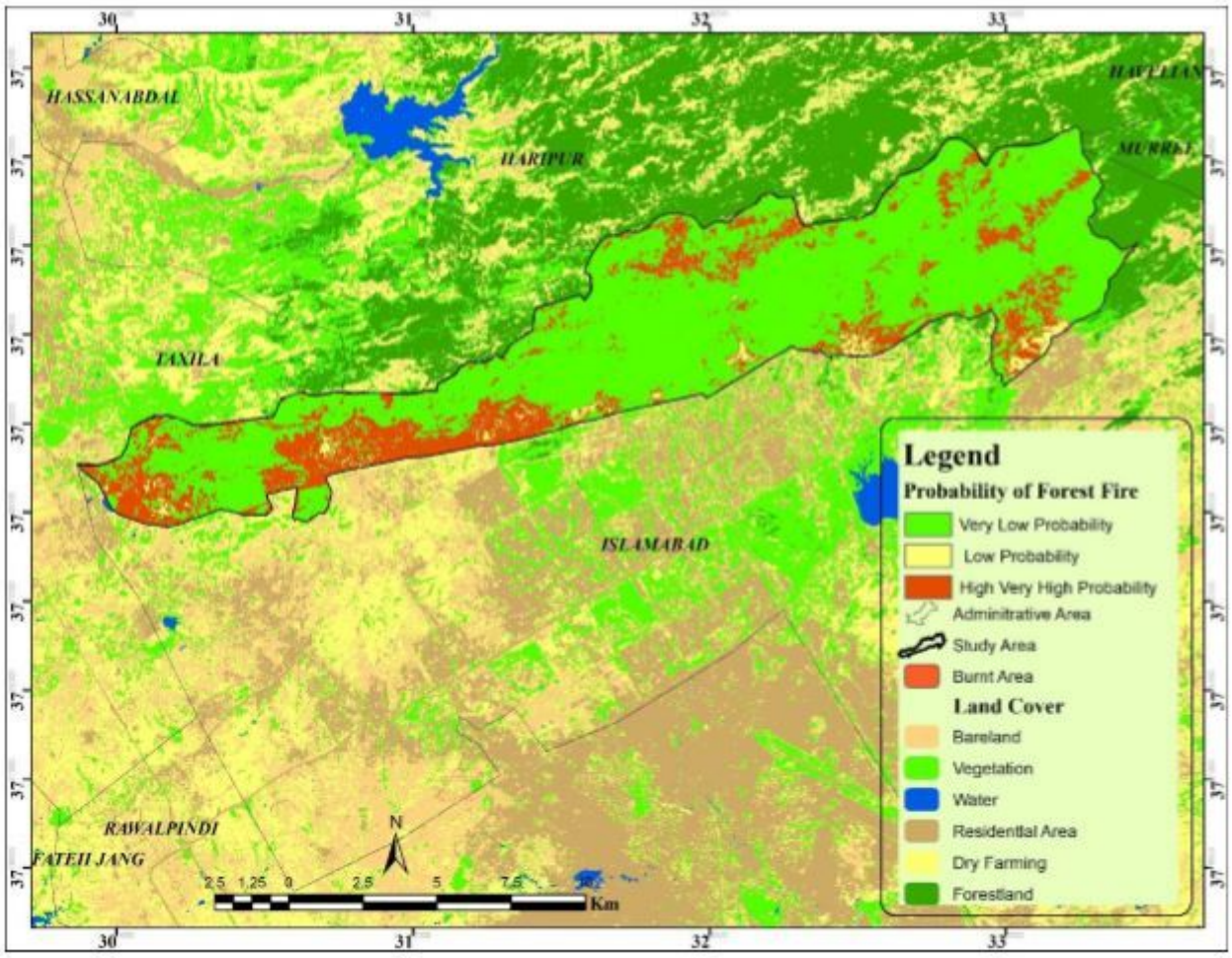

Figure 10

Susceptibility map of spreading forest fires.